

# METODOLOGIJA ODREĐIVANJA KORISNIČKE POGONSKE KARTE HIDROAGREGATA METHODOLOGY FOR DETERMINING THE ACTUAL PQ DIAGRAM OF A HYDROGENERATOR

Prof. emer. dr. sc. Ivan Ilić, prof. dr. sc. Zlatko Maljković, prof. dr. sc. Ivan Gašparac, mr. sc. Milutin Pavlica, mr. sc. Dubravka Ilić-Zubović, Vladimir Jarić, dipl. ing., Sveučilište u Zagrebu, Fakultet elektrotehnike i računarstva, Unska 3, 10000 Zagreb, Hrvatska  
Doc. dr. sc. Alfredo Višković, HEP d.d.,  
Ulica grada Vukovara 37, 10000 Zagreb, Hrvatska  
Radivoj Belobrajčić, dipl. ing., HEP Proizvodnja d.o.o., PP HE Zapad,  
Eugena Kumičića 13, 51000 Rijeka, Hrvatska

U radu je predložena metodologija određivanja korisničke pogonske karte kao ključnog dokumenta svake proizvodne jedinice električne energije. Opisane su sve granice od kojih se sastoji pogonska karta hidrogeneratora. Detaljno su izložene teorijske podloge na kojima leže postupci za njihovo određivanje. Poseban osvrt je dan manje istraženom problemu zagrijavanja čeonog prostora hidrogeneratora. Pregledno je prikazan i obrazložen slijed postupaka koji sačinjavaju metodologiju. Detaljne analize i proračuni, posebno korištenjem suvremenih numeričkih programskih alata, daju dobar uvid u mogućnosti rada generatora i mogu poslužiti kao priprema za ispitivanja i mjerenja. Rezultati dobiveni mjerenjima i ispitivanjima obrađuju se i tumače, te se tek na osnovi tako dobivenih rezultata sa sigurnošću određuju granice dozvoljenog rada generatora. Konačan rezultat provođenja ispitivanja prema predloženoj metodologiji je korisnička pogonska karta: stvarna, mjerenjem potvrđena pogonska karta hidrogeneratora.

This paper presents the methodology for determining the actual PQ diagram as a key document for any power generation unit. It describes all the limits of which a hydrogenerator PQ diagram consists. There is a detailed explanation of the theoretical basis of the procedures for their determination. It also contains a reference to the less researched problem of heating in the hydrogenerator end region. The paper clearly shows and explains the sequence of the procedures which make up the methodology. Detailed analyses and calculations, particularly using modern numerical programming tools, provide a good insight in generator performance and may serve as a preparation for testing and measuring. The measurement and testing data is processed and interpreted, and it is only on the basis of the results thus established that the limits for the permitted operation of the generator are positively determined. The final result of the testing conducted in accordance with the methodology proposed is the actual PQ diagram: the real PQ diagram of the hydrogenerator, confirmed by the measurement.

**Ključne riječi:** čeonni prostor, hidrogenerator, pogonska karta, sinkroni generator, zagrijavanje  
**Keywords:** end region, heating, hydrogenerator, PQ diagram, synchronous generator







## 1 UVOD

Pogonska karta (pogonski dijagram) hidrogeneratora ključni je dokument svakog hidrogeneratora koji je priključen na elektroenergetski sustav [1], [2] i [3]. U novijim elektranama danas postoje računalni zasloni na kojima je prikazana pogonska karta s osvijetljenom točkom trenutnog radnog stanja generatora. No s druge strane, praksa pokazuje da granice dopuštenog rada vrlo često ne odgovaraju stvarnim svojstvima i mogućnostima hidrogeneratora.

S obzirom na podloge za crtanje pogonske karte, razlikuju se proizvođačka, eksploatacijska i korisnička (aktualna) pogonska karta. Proizvođač generatora jamči da će isporučeni generator moći trajno raditi u ugovorenim dozvoljenim područjima rada prikazanim odgovarajućim P-Q dijagramom, proizvođačkom pogonskom kartom.

Za razliku od nje, korisnička pogonska karta određuje se tako što se istražuju mogućnosti rada generatora i izvan dozvoljenog područja rada definirano od strane proizvođača. Kod novih generatora ovakvi postupci mogu otkriti proširenje dozvoljenog područja rada zbog potencijala generatora koji nisu ugovoreni s proizvođačem. Kod generatora koji su dulje vrijeme u pogonu ponovo određena pogonska karta može ukazati na smanjenje dozvoljenog područja rada zbog starenja dijelova generatora.

U ovom se članku objašnjavaju postupci koji uključuju i specijalistička mjerenja, točnijeg određivanja aktualne pogonske karte hidrogeneratora, odnosno hidroagregata, kao i hidroagregata s uključenim blok-transformatorom [4] i [5].

## 1 INTRODUCTION

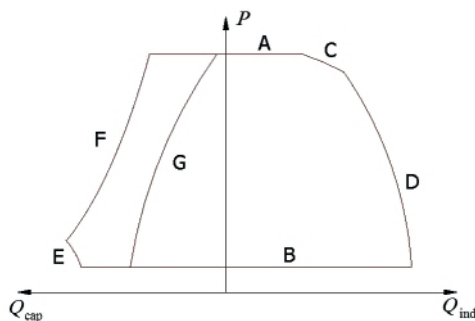
The PQ diagram of a hydrogenerator is the key document of any hydrogenerator connected into the power supply system [1], [2] and [3]. In newer power plants today, there are computer screens showing the PQ diagram with an illuminated point indicating the current operating state of the generator. On the other hand, practice shows that the limits of the permitted operation very often do not correspond with the real characteristics and performance of a hydrogenerator.

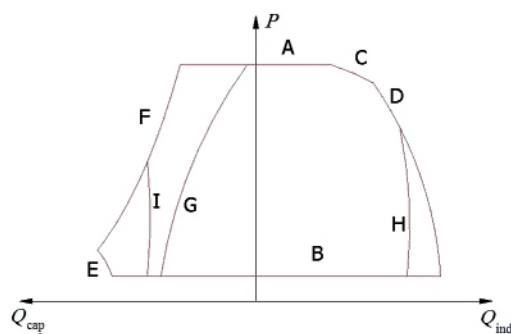
Considering the basis for the PQ diagram, we distinguish between the manufacturer's, operating and actual (user) PQ diagrams. The manufacturer of a generator guarantees that the generator delivered will be able to constantly operate within the agreed and permitted range presented in the appropriate (manufacturer's) PQ diagram.

The actual PQ diagram, however, is determined through the testing of the generator's operating capability beyond the permitted operating domain defined by the manufacturer. In new generators such proceeding may result in a broadening of the permitted operating domain owing to the newly found potentials of the generator which had originally not been agreed with the manufacturer. In generators which have been in operation for some time, a new PQ diagram may indicate a reduction in the permitted operating domain due to the ageing of generator parts.

This paper explains the procedures which also include specialist measurements, more accurate determination of the actual PQ diagram of the hydrogenerator, i.e. the generator-turbine unit, as well as the generator-turbine unit with the block transformer [4] and [5].

**Slika 1**  
Granice pogonske karte  
hidroagregata  
(turbina + generator)  
Figure 1  
Limits of a PQ diagram  
of the turbine-generator  
unit





**Slika 2**  
 Granice pogonske karte hidroagregata na pragu elektrane (turbina + generator + blok-transformator)  
**Figure 2**  
 Limits of a PQ diagram of the power plant threshold unit (turbine + generator + block transformer)

Na slici 1 prikazana su ograničenja nastala zbog:

- A – maksimalne snage pogonskog stroja,
- B – minimalne snage pogonskog stroja,
- C – zagrijavanja statorskog namota,
- D – zagrijavanja uzbuđnog namota,
- E – minimalne uzbude,
- F – praktične granice statičke stabilnosti,
- G – zagrijavanja čeonog prostora.

Figure 1 shows restrictions due to:

- A – maximum machine power,
- B – minimum machine power,
- C – heating of stator winding,
- D – heating of excitation winding,
- E – minimum excitation,
- F – practical limit of static stability,
- G – heating of end region.

Na slici 2 dodane su granice karakteristične za pogonsku kartu agregata s blok transformatorom (PK na pragu elektrane) koje slijede iz ograničenja zbog:

- H – maksimalnog napona armature generatora,
- I – minimalnog napona armature generatora.

In Figure 2, the limits characteristic of a PQ diagram of the unit with the block transformer (PQ at power plant threshold) are added, which follow from the restrictions due to:

- H – maximum voltage of generator armature,
- I – minimum voltage of generator armature.

## 2 KORISNIČKA POGONSKA KARTA

Korisnička (stvarna, aktualna) pogonska karta (KPK) je, u svom pretežitom dijelu, toplinski dijagram [6], u kojem glavne teoretske krivulje predstavljaju maksimalno dopušteno zagrijavanje različitih aktivnih dijelova sinkronog generatora. Na slikama 1 i 2 granica statorske struje predstavlja maksimalno zagrijavanje statorskog namota (C), granica struje uzbude predstavlja maksimalno zagrijavanje namota rotora (D), granica kapacitivnog rada predstavlja maksimalno zagrijavanje elemenata stroja u čeonom prostoru (zubi, tlačni prsti, tlačna ploča) (G).

Na korisničkom pogonskom dijagramu su, osim termičkih, prikazane još i sljedeće granice :

## 2 ACTUAL PQ DIAGRAM

The actual PQ diagram (APQ) is, for the most part, a thermal diagram [6] in which the main theoretical curves show the maximum permitted heating of different active parts of the synchronous generator. In Figures 1 and 2 the limit of the stator current represents the maximum heating of the stator winding (C), the limit of the excitation current represents the maximum heating of the rotor winding (D), the limit of the capacitive operation represents the maximum heating of the machine elements in the end region (teeth, pressure fingers, pressure plate) (G).

In addition to the thermal limits, the actual PQ also shows the following limits:

- granica maksimalne radne snage zbog ograničenja u radu hidrauličke turbine, odnosno hidrauličkog trakta (A),
- granica minimalne radne snage zbog ograničenja u radu hidrauličke turbine, odnosno hidrauličkog trakta (B),
- granica minimalne uzbudne struje zbog ograničenja uzbudnog sustava, regulatora napona i generatorskih zaštita (E),
- granica statičke stabilnosti s rezervom od 10 % (F), koja može biti restriktivnija od toplinske granice čeonog prostora.

Pogonska karta agregata s blok-transformatorom (slika 2) crta se za konstantan napon na visokonaponskoj (VN) strani blok-transformatora, pa se mogu pojaviti i dodatna ograničenja koja slijede iz definiranih ograničenja dopuštenog radnog napona generatora.

U idealnom slučaju, za nove generatore ili generatore koji su imali lakši režim rada (u baznim elektranama elektroenergetskog sustava) proizvođačka, eksploatacijska i aktualna pogonska karta su gotovo identične.

Toplinske se granice, za određenu toplinsku klasu izolacije, mogu odrediti mjerenjem napona, struje, snage i pripadnih dopuštenih zagrijavanja u statorskom i rotorskom namotu, statorskom paketu i limovima krajnjih zubi u temperaturno ustaljenim pogonskim stanjima.

- maximum operating power limit due to operating limitations of the hydraulic turbine i.e. hydraulic tract (A),
- minimum operating power limit due to operating limitations of the hydraulic turbine i.e. hydraulic tract (B),
- minimum excitation current limit due to the limitations of the excitation system, voltage regulator and generator protection (E),
- static stability limit with 10 % reserve (F), which may be more restrictive than the thermal limit of the end region.

A PQ diagram of the unit with the block transformer (Figure 2) is drawn for the constant voltage at the high-voltage (HV) side of the block transformer, so there may also be additional limitations which follow from the definite limitations of the permitted operating voltage of the generator.

Ideally, in new generators and generators which have run under an easier operating regime (at base-load power plants in the power generation system), the manufacturer's, operating and actual PQs are nearly identical.

The thermal limits for a particular thermal insulation class may be determined by measuring the voltage, current, power and permitted heating in the stator and rotor windings, the stator package and the sheet-metal strips of the end teeth in thermally steady operating conditions.

### 3 OPĆI PRISTUP ODREĐIVANJU KORISNIČKE POGONSKE KARTE

#### 3.1 Pristup određivanju korisničke pogonske karte sinkronog agregata

Određivanje KPK sinkronog agregata, uključivo s blok-transformatorom, treba zasnivati na sljedećim podlogama i dokumentaciji dostupnoj korisniku:

- projektnoj dokumentaciji turbine, generatora i transformatora,
- protokolima ispitivanja pri izradi i pri puštanju u pogon turbine, generatora i transformatora,
- ispitnoj dokumentaciji dobivenoj pri remontu i neplaniranim intervencijama,
- zapažanjima korisnika pri pogonu u stacionarnom radu i pri prijelaznim pojavama,
- naknadno rađenim elaboratima o bilo kojoj problematici vezanoj uz generator, turbinu i transformator.

### 3 GENERAL APPROACH TO DETERMINING THE ACTUAL PQ DIAGRAM

#### 3.1 Approach to determining the actual PQ diagram for the synchronous unit

Determining the APQ for the synchronous unit, including the block transformer, should be based on the following materials and documents available to the user:

- project documentation of the turbine, generator and transformer,
- test protocols prepared during the construction and commissioning of the turbine, the generator and the transformer,
- test documentation from overhaul and contingent interventions,
- observations of the user during the stationary operation and in the cases of transitional occurrences,
- subsequent papers on any problem related to the generator, the turbine and the transformer.

Ovisno o kompletnosti prikupljene dokumentacije, na generatoru treba obaviti:

- dodatna ispitivanja koja je moguće obaviti bez ugradnje dodatnih davača u sam generator:
  - pokus praznog hoda,
  - pokus kratkog spoja,
  - specijalistička ispitivanja kojima se određuju ili provjeravaju sumnjivi parametri,
- specijalistička ispitivanja koja se mogu obaviti tek nakon ugradnje Hallovihi sondi, termosondi i akcelerometara, a uključuju i pokuse praznog hoda i kratkog spoja:
  - magnetska mjerenja radijalne i aksijalne komponente indukcije u karakterističnim točkama stroja,
  - toplinska točkasta mjerenja u karakterističnim dijelovima stroja,
  - mjerenje kuta opterećenja,
  - mjerenja vibracija u karakterističnim točkama stroja.

U sljedećoj fazi treba, što je moguće detaljnije, analizirati sve prikupljene rezultate proračuna i mjerenja, a posebno valja obratiti pozornost na sljedeće fizikalne veličine i parametre:

- uzbudnu struju praznog hoda  $I_{0p}$ ,
- uzbudnu struju praznog hoda nezasićenog generatora  $I_{0g}$ ,
- uzbudnu struju kratkog spoja  $I_{0k}$ ,
- sinkronu reaktanciju u uzdužnoj osi  $x_d$ ,
- sinkronu reaktanciju u poprečnoj osi  $x_q$ ,
- kratkospojni omjer  $k_c$ ,
- rasipnu reaktanciju armature  $x_\sigma$ .

Poželjno je imati osnovne informacije o specifičnim magnetskim i električnim opterećenjima, što će pomoći u kasnijoj analizi:

- indukcije u praznom hodu i pri nazivnom opterećenju na sljedećim mjestima:
  - u zračnom rasporu  $B_\delta$ ,
  - u zubi statora  $B_{zs}$ ,
  - u jarmu statora  $B_{js}$ ,
  - u polu rotora  $B_p$ ,
  - na ostalim mjestima gdje je povećana indukcija zbog neke nestandardne izvedbe (npr. u lastinom repu korijena pola, u jarmu rotora i slično),
- strujnog obloga, odnosno protjecanja armature i uzbude za nazivno opterećenje te
- parcijalnih gubitaka.

Za transformator je potrebno imati osnovne podatke i, po mogućnosti mjerenjem potvrđen, napon kratkog spoja ( $u_k$ ). Ako postoje odvojci na

Depending on how complete the collected documentation is, the following should be done with the generator:

- additional tests which can be conducted without installing additional sensors in the generator itself:
  - no-load test,
  - short circuit test,
  - specialist testing to determine or check suspicious parameters,
- specialist testing which can only be conducted after Hall probes, thermal probes and accelerometers have been installed, including no-load and short circuit tests:
  - magnetic measurement of the radial and axial components of induction at characteristic machine points,
  - hotspot measurements in characteristic machine parts,
  - measurement of load angle,
  - measurement of vibrations at characteristic machine points.

In the next phase it is necessary to analyse, as closely as possible, all the calculations and measurements collected, paying particular attention to the following physical values and parameters:

- no-load excitation current  $I_{0p}$ ,
- no-load excitation current for the non-saturated generator  $I_{0g}$ ,
- short circuit excitation current  $I_{0k}$ ,
- synchronous reactance at the longitudinal axis  $x_d$ ,
- synchronous reactance at the transversal axis  $x_q$ ,
- short circuit ratio  $k_c$ ,
- leakage reactance of the armature  $x_\sigma$ .

It is desirable to have the basic information about specific magnetic and electrical loads, which will be of help in the subsequent analysis of:

- induction at no load and at nominal load in:
  - air gap  $B_\delta$ ,
  - stator tooth  $B_{zs}$ ,
  - stator yoke  $B_{js}$ ,
  - rotor pole  $B_p$ ,
  - in other places where induction is increased owing to some non-standard design (e.g. in the pole root swallowtail, rotor yoke, and alike),
- current covering, i.e. armature flux and excitation at the rated load, and
- partial losses.

For the transformer it is necessary to have the basic data and short-circuit voltage ( $u_k$ ), if possible

transformatoru, treba poznavati te podatke za sve moguće prijenosne omjere, te na kojem je položaju postavljen premještač.

Najsloženiji i najosjetljiviji korak predstavljaju pripreme i mjerenja vezana uz čeonu prostor generatora. Pripreme se sastoje od izbora i umjeravanja Hallovih sondi i termosondi, te pažljivoj ugradnji na ključna mjesta, do usklađivanja mogućih termina izvođenja mjerenja na hidrogeneratoru.

Konačna analiza specijalističkih mjerenja završava određivanjem koeficijenta međuveze ( $k_A$ ) između uzbudnog protjecanja i aksijalne komponente magnetskog polja na osnovi mjerenja provedenih na ključnim mjestima u čeonom prostoru i na kraju iscrtavanjem granice zagrijavanja krajnjih limova i eventualno drugih dijelova u čeonom prostoru u kapacitivnom radu generatora.

Paralelna mogućnost određivanja elektromagnetskih i toplinskih prilika u čeonom prostoru sastoji se u korištenju mjerenjem dobivenih podataka o raspodjeli uzdužne komponente magnetske indukcije i njihovoj usporedbi s raspodjelom dobivenom numeričkim računom uz pomoć metode konačnih elemenata (MKE); ukoliko se pokaže računom dobivena razdioba pouzdanom za određeni tip konstrukcije generatora, tj. dovoljno točnom u odnosu na mjerenjem dobivene rezultate, to se daljnje analize mogu provoditi korištenjem numeričkog računa. Ovakav pristup omogućava projektantu i konstruktoru generatora sigurnije projektiranje s obzirom na probleme povećanog zagrijavanja krajnjih limova paketa statora u čeonom prostoru stroja.

Sljedeći korak predstavlja iscrtavanje pogonske karte sa svim ograničenjima. U konačnici, to iscrtavanje treba biti automatizirano interaktivnim programskim paketom, u kojem osnovne veličine i parametre treba direktno upisivati.

### 3.2 Ključni parametri za određivanje i crtanje korisničke pogonske karte agregata

Parametri ključni za određivanje KPK hidroagregata za nominalni napon generatora  $U_n$  su:

- maksimalna snaga turbine, nazivna snaga i korisnost generatora  $P_T$ ,  $P_n$ ,  $\eta_G$  (iz dokumentacije generatora i turbine),
- minimalna snaga turbine  $P_{Tmin}$  (iz dokumentacije turbine),
- maksimalno dozvoljeno zagrijavanje statorskog namota  $S_n$ ,  $v_p$ ,  $v_s$  (iz dokumentacije generatora), gdje su  $v_s < 1$  i  $v_p > 1$  koeficijenti sniženja, odnosno povišenja napona, što se određuje

confirmed by measurement. If there are taps on the transformer, it is necessary to know such a data for any possible transformation ratios, and in what position the changer is placed.

The most complex and sensitive steps are preparations and measurements related to the end region of the generator. Preparations range from the selection and calibration of the Hall probes and thermal probes, and their careful installation at key locations, to the harmonisation of the possible scheduling for the measurements to be performed on the hydrogenerator.

The final analysis of specialist measurements closes with the determination of the coefficient of interrelation ( $k_A$ ) between the excitation flux and the axial component of the magnetic field based on the measurements conducted at the key locations in the end region, and finally by plotting the thermal limit for end sheet-metal strips and possibly other parts in the end region during the capacitive operation of the generator.

A parallel possibility to determine the electromagnetic and thermal conditions in the end region includes the measurement data about the distribution of the longitudinal component of the magnetic induction and its comparison with the distribution obtained from the numerical calculation using the finite element method (FEM); should the distribution obtained by the calculation prove reliable for a particular type of generator design, i.e. accurate enough compared with the results obtained by measurement, further analyses may be conducted using the numerical calculation. Such an approach gives the generator designer and constructor more security with regard to the problems of increased heating of end sheet-metal strips of the stator package in the end region of the machine.

The next step is to plot the PQ diagram with all the limitations. This plotting should actually be automated by means of an interactive software package in which all the values and parameters need to be entered directly.

### 3.2 Key parameters for determining and plotting the actual PQ diagram of the power generation unit

The key parameters for determining the APQ of the hydrogenerator unit for the rated generator voltage  $U_n$  are:

- maximum turbine power and related generator power and efficiency  $P_T$ ,  $P_n$ ,  $\eta_G$  (from generator and turbine documentation),
- minimum turbine power  $P_{Tmin}$  (from turbine documentation),

- ugovorom između proizvođača generatora i kupca,
- zagrijavanje uzbuđenog namota (iz dokumentacije generatora i mjerenja u praznom hodu i kratkom spoju)  $X_d, X_q, E_{max}, v_i, \delta_i$ , gdje je  $v_i$  koeficijent sniženja, odnosno povišenja napona, što se određuje ugovorom između proizvođača generatora i kupca, a  $E_{max}$  najveća vrijednost induciranog napona,
  - minimalna uzbudna struja  $E_{min}, k, E_{max}$  (iz dokumentacije generatora i/ili mjerenja) gdje je  $k$  omjer minimalne i maksimalne uzbudne struje,
  - praktična granica stabilnosti  $X_d, X_q$  (iz dokumentacije generatora ili mjerenja).

- maximum permitted heating of stator winding  $S_n, v_p, v_s$  (from generator documentation), whereas  $v_s < 1$  and  $v_p > 1$  are coefficients of decrease or increase in voltage, as agreed between the manufacturer of the generator and the customer,
- heating of the excitation winding (from generator documentation and no-load and short circuit measurements)  $X_d, X_q, E_{max}, v_i, \delta_i$ , whereas  $v_i$  is the coefficient of decrease or increase in voltage, as determined by agreement between the manufacturer of the generator and the customer, and  $E_{max}$  the highest value of induced voltage,
- minimum excitation current  $E_{min}, k, E_{max}$  (from generator documentation and/or measurement) whereas  $k$  is the ratio between the minimum and the maximum excitation currents,
- practical stability limit  $X_d, X_q$  (from generator documentation or measurement).

## 4 GRANICE KORISNIČKE POGONSKE KARTE

### 4.1 Ograničenje rada generatora zbog maksimalne i minimalne snage pogonskog stroja

U pogonsku kartu treba ucrtati stvarnu granicu maksimalne i minimalne snage koja je definirana mogućnošću pogonskog stroja – turbine. Tako će ograničenje maksimalne snage biti definirano dvojako, ovisno o odnosu snage turbine i nazivne djelatne snage generatora. Ako je snaga turbine veća od nazivne djelatne snage generatora  $P_T > P_n$ , tada je:

$$P_{max} = P_n \cdot \quad (1)$$

Ako je snaga turbine jednaka ili manja od nazivne djelatne snage generatora  $P_T \leq P_n$ , tada je:

$$P_{max} = P_T \cdot \eta_G \cdot \quad (2)$$

Minimalna snaga u pogonskoj karti ograničena je samo zahtjevima turbine, odnosno hidrauličkog trakta. Kod nekih vrsta turbina tog ograničenja nema (Pelton turbina), dok kod drugih (Kaplan, Francis itd.) minimalna snaga je u granicama od 5 % do 30 % nazivne snage. Kako to ograničenje nije definirano u preciznim granicama, dovoljno je u pogonsku kartu agregata ucrtati kao minimalnu snagu onu, koju određuje turbina ili točnije

## 4 LIMITS OF ACTUAL PQ DIAGRAM

### 4.1 Limitation of generator operation on account of the maximum power and the minimum power of the machine

PQ diagram needs to plot the actual limit of the maximum and minimum powers as defined by the performance of the machine – the turbine. This way the limitation of the maximum power will be defined twofold, depending on the relation between the power of the turbine and the rated power of the generator. If the power of the turbine exceeds the power of the generator  $P_T > P_n$ , then:

If the power of the turbine is equal to or lower than the rated power of the generator  $P_T \leq P_n$ , then:

The minimum power in the PQ diagram is only limited by the requirements of the turbine, i.e. the hydraulic tract. In some types of turbines this limitation does not exist (Pelton turbine), whereas in others (Kaplan, Francis etc.) the minimum output remains within 5 % to 30 % of the rated output. Because this limitation is not defined within any precise limits, it is sufficient to plot into the PQ diagram of the unit as its minimum power, the value



uzimajući u obzir i korisnost generatora za navedenu snagu, odnosno:

of the power determined by the turbine or, more accurately, by also taking into account the efficiency of the generator for the power mentioned, that is:

$$P_{\min} = P_{T\min} \cdot \eta_G. \quad (3)$$

Ove granice se u pogonski dijagram ucrtavaju kao pravci  $P = P_{\max}$  i  $P = P_{\min}$ .

These limits are plotted into the PQ diagram as lines  $P = P_{\max}$  and  $P = P_{\min}$ .

#### 4.2 Ograničenje rada generatora zbog zagrijavanja namota statora

U realnom elektroenergetskom sustavu napon mreže nije krut, pa ni napon generatora nije stalno jednak nazivnom. Zato je generator obično projektiran i izveden za rad s naponima nešto višim ( $U_3$ ) i nešto nižim ( $U_1$ ) od nazivnoga, pri čemu se nominalna snaga ne mijenja:

#### 4.2 Limitation of generator operation on account of the heating of the stator winding

In a real power generation system the network voltage is not rigid, so the voltage of the generator does not constantly equal the rated voltage. This is why the generator is usually designed and constructed to operate with slightly higher ( $U_3$ ) and slightly lower ( $U_1$ ) than rated voltages, without affecting the rated power:

$$U_1 = v_s \cdot U_n; v_s < 1, \quad (4)$$

$$U_3 = v_p \cdot U_n; v_p > 1. \quad (5)$$

Generator bi za svaki napon u granicama  $U_1$  do  $U_3$  morao moći davati u mrežu nazivnu prividnu snagu  $S_n$ . Iz tog uvjeta slijedi (sve veličine su u p.u.):

For any voltage within the limits of  $U_1$  to  $U_3$  the generator should be able to deliver the rated apparent power  $S_n$  to the network. From this requirement follows (all the values are p.u.):

$$I_1 = \frac{S_n}{U_1}, \quad (6)$$

$$I_2 = \frac{S_n}{U_n} = I_n, \quad (7)$$

$$I_3 = \frac{S_n}{U_3}, \quad (8)$$

$$I_{\max} = \max \{I_1, I_2, I_3\} = I_1. \quad (9)$$

Uz pomoć te struje maksimalnog iznosa moguće je naći granice zagrijavanja namota statora koje odgovaraju trima karakterističnim točkama:

– sniženog napona:

With the help of this maximum current it is possible to find the limits of the heating of the stator winding for the three characteristic points:

– lower voltage:

$$U = U_1, \quad S_1 = I_{\max} \cdot U_1 = S_n, \quad (10)$$

– nazivnog napona:

– rated voltage:

$$U = U_2, \quad S_2 = I_{\max} \cdot U_n = \frac{S_n}{v_s}, \quad (11)$$

– i povišenog napona:

– and higher voltage:

$$U = U_3, \quad S_3 = I_n \cdot U_3 = S_n \cdot v_p. \quad (12)$$

Proizvođač jamči da generator može trajno u mrežu davati nazivnu prividnu snagu ( $S_n$ ), uz sniženi ( $U_1$ ) i povišeni ( $U_3$ ) napon. Rashladni sustav generatora mora biti u stanju odvesti dodatnu toplinu proizvedenu u armaturnom namotu zbog povećane struje armature (pri sniženom naponu i nazivnoj prividnoj snazi), te biti u stanju odvesti dodatnu toplinu stvorenu uslijed gubitaka u željezu zbog povišenog napona (uz nazivnu prividnu snagu i armaturnu struju manju od nazivne). Međutim, to ne znači da mora jamčiti istodobni rad s najvećim dozvoljenim naponom i najvećom dozvoljenom strujom. Stoga se pri povišenom naponu dozvoljava rad s nazivnom armaturnom strujom, a ne maksimalno dozvoljenom. Pri tome se ne smije zaboraviti ni utjecaj uzbudnih gubitaka, koji ovise o uzbudnoj struji za svako od spomenutih radnih stanja. Stvarna granica može se odrediti isključivo mjerenjem zagrijavanja stroja na pažljivo odabranim mjestima.

Granica zagrijavanja se ucrtava u pogonsku kartu kao polukružnica (krivulje C na slikama 1 i 2) sa centrom u ishodištu i polumjerom  $S_r$ .

The manufacturer guarantees that the generator can permanently deliver the rated apparent power ( $S_n$ ) to the network, with lower ( $U_1$ ) and higher ( $U_3$ ) voltage. The cooling system of the generator must be capable of eliminating the additional heat generated in the armature winding due to the stronger armature current (at lower voltage and rated apparent power), as well as of eliminating the additional heat generated because of the losses in iron caused by higher voltage (at the rated apparent power and armature current lower than rated). However, this does not mean that it must guarantee simultaneous operation at the highest permitted voltage and the highest permitted current. This is why at higher voltage it is permitted to operate at the rated armature current, and not at the maximum permitted current. One should not forget the effect of excitation losses either, which depend on the excitation current for each of the mentioned operating conditions. The actual limit can be determined by measuring the heating of the machine at carefully selected places.

The heating limit is plotted into the PQ diagram as a semi-circle (C-curves in Figures 1 and 2) with its centre at the originating point and radius  $S_r$ .

#### 4.3 Ograničenje rada generatora zbog zagrijavanja namota uzbuđe ( $I_{fmax}$ )

Maksimalna uzbuđa određuje se sličnim postupkom kao i maksimalna armaturna struja. Uvjet je da generator može raditi u nazivnoj radnoj točki uz sva tri napona armature. Maksimalna se uzbuđa određuje kao najveća uzbuđa. Pritom za generator s istaknutim polovima vrijedi izraz (sve veličine su u p.u.):

$$\frac{E \cdot U}{X_d} = \frac{P}{\sin \delta} - \frac{U^2}{2} \cdot \frac{X_d - X_q}{X_d \cdot X_q} \cdot \frac{\sin(2\delta)}{\sin \delta}, \quad (13)$$

gdje je:

$$\operatorname{tg} \delta = \frac{P}{\frac{U^2}{X_q} + Q}. \quad (14)$$

U karakterističnim je točkama:

$$U_i = v_i \cdot U_n, \quad (15)$$

$$\operatorname{tg} \delta_i = \frac{P_n}{\frac{v_i^2 \cdot U^2}{X_q} + Q_n}, \quad (16)$$

$$E_i = \frac{X_d}{v_i \cdot U_n} \cdot \left( \frac{P_n}{\sin \delta_i} - v_i^2 \cdot U_n^2 \cdot \frac{X_d - X_q}{X_d \cdot X_q} \cdot \cos \delta_i \right). \quad (17)$$

Iz navedenog slijedi da je granica zbog maksimalne uzbuđe određena s:

$$E_{max} = \max \{E_i\}. \quad (18)$$

Parametar  $v_i$  odabire se kao onaj od parametara  $v_s$  i  $v_p$  za koji se dobije maksimum napona  $E_i$ .

#### 4.3 Limitation of generator operation on account of the heating of the excitation winding ( $I_{fmax}$ )

The maximum excitation is determined in a similar procedure as the maximum armature current. The condition is that at the rated operating point the generator can operate at all three armature voltages. The maximum excitation is determined as the highest excitation. To the generator with pronounced poles the following expression is applicable (all the values are p.u.):

whereas:

In the characteristic points:

It follows that the limit, due to the maximum excitation, is determined by:

Parameter  $v_i$  is selected as parameter  $v_s$  or  $v_p$  for which the maximum voltage  $E_i$  is obtained.





$$E_{\min} = k \cdot E_{\max}, \quad (19)$$

gdje je  $k$  koeficijent, najčešće u granicama od 0 do 0,3.

whereas  $k$  is the coefficient, mostly within the limits from 0 to 0.3.

#### 4.5 Ograničenje rada generatora zbog praktične granice statičke stabilnosti

U pogonsku je kartu još potrebno ucrtati i praktičnu granicu stabilnosti (PGS) [10], [11] i [12], koja se konstruira tako da se ucrtaju nekoliko krivulja konstantne uzbuđene (opisano u 4.4) i da se iz tjemena svake krivulje konstantne uzbuđene (teorijska granica stabilnosti) spusti za  $0,1 \cdot S_n$ , te se pospaja dobivene točke glatkom krivuljom (slika 3).

Drugi se način određivanja granice stabilnosti egzaktno može opisati slijedećim postupkom:

Pri izvodu izraza za praktičnu granicu stabilnosti polazi se od relacija koje daju ovisnost djelatne i jalove snage o kutu opterećenja za generator sa istaknutim polovima (sve veličine su u p.u.):

#### 4.5 Limitation of generator operation on account of the practical limit of static stability

It is also necessary to plot into the PQ diagram the practical limit of stability (PGS) [10], [11] and [12], which is created by plotting several curves for the constant excitation (described in 4.4), lowered from the vertex of each constant excitation curve (theoretical limit of stability) by  $0,1 \cdot S_n$ , and connecting all the points with a smooth curve (Figure 3).

Another way to determine the limit of stability can be accurately described by the following procedure:

In deriving the expression for the practical limit of stability, one is to start from the relations which show the dependence of the real and reactive power on the load angle for the generator with pronounced poles (all the values are p.u.):

$$P = \frac{E \cdot U}{X_d} \sin \delta + \frac{U^2}{2} \cdot \frac{X_d - X_q}{X_d \cdot X_q} \sin 2\delta, \quad (20)$$

$$Q = \frac{E \cdot U}{X_d} \cos \delta + U^2 \cdot \frac{X_d - X_q}{X_d \cdot X_q} \cos^2 \delta - \frac{U^2}{X_q}. \quad (21)$$

Teorijska granica stabilnosti (TGS) je skup onih točaka kod kojih se za neku uzbuđenu (koja ovdje predstavlja parametar) postiže maksimalna djelatna snaga (pri prekretnom kutu). Prekretni kut dobiva se iz uvjeta:

The theoretical limit of stability (TGS) is a set of points in which the maximum real power (at breakover angle) is achieved for the excitation (which is here a parameter). The breakover angle results from the condition:

$$\frac{dP}{d\delta} = \frac{E \cdot U}{X_d} \cdot \cos \delta + U^2 \cdot \frac{X_d - X_q}{X_d \cdot X_q} \cos(2\delta) = 0. \quad (22)$$

Rješenjem te jednadžbe po kutu dobiva se prekretni kut, pa se može dobiti parametarski oblik krivulje teorijske granice stabilnosti:

Solving this equation by angle gives the breakover angle, in order to obtain the parametric form of the curve of the theoretical stability limit:

$$P = a \cdot \sqrt{\frac{1}{2} - 2 \cdot s^2 + 2 \cdot s \cdot \sqrt{s^2 + \frac{1}{2}}} \cdot \left( 3 \cdot s + \sqrt{s^2 + \frac{1}{2}} \right), \quad (23)$$

$$Q = a \cdot \left( \frac{1}{2} - 2 \cdot s^2 + 2 \cdot s \cdot \sqrt{s^2 + \frac{1}{2}} \right) + Q_0, \quad (24)$$

gdje su:

whereas:

$$s = \frac{E}{4 \cdot U} \cdot \frac{X_q}{X_d - X_q}, \quad (25)$$

$$a = U^2 \cdot \frac{X_d - X_q}{X_d \cdot X_q}, \quad (26)$$

$$Q_0 = \frac{U^2}{X_q}. \quad (27)$$

Jednadžbe (23) i (24) predstavljaju parametarski oblik krivulje teorijske granice stabilnosti.

Equations (23) and (24) represent the parametric form of the curve of the theoretical stability limit.

Kod izvođenja izraza za praktičnu granicu stabilnosti potrebna je jednadžba krivulje konstantne uzbuđenja, koja glasi:

In deriving the expression for the practical stability limit, the equation of the constant excitation curve is necessary:

$$\left[ P^2 + (Q - Q_0)^2 \right]^2 - \left[ P^2 + (Q - Q_0)^2 \right] \cdot \left[ (4as)^2 + 2a(Q - Q_0) \right] + a^2(Q - Q_0)^2 = 0. \quad (28)$$

U gornjim je jednadžbama parametar uzbuđenja  $E$ , odnosno njoj proporcionalna veličina  $s$ . Za neku vrijednost parametra  $s$ , vrijednost koordinate  $P$  dobije se tako da se od vrijednosti koja se dobije iz teoretske prekritne snage oduzme 0,1 p.u.:

In these equations the parameter is excitation  $E$ , i.e. value  $s$  that is proportionate to it. As the value of parameter  $s$ , the value of coordinate  $P$  is obtained by deducting 0.1 p.u. from the value arrived at from the theoretical breaker power:

$$P_p = a \sqrt{\frac{1}{2} - 2s^2 + 2s \sqrt{s^2 + \frac{1}{2}}} \cdot \left( 3s + \sqrt{s^2 + \frac{1}{2}} \right) - 0,1. \quad (29)$$

Parametarski oblik praktične granice stabilnosti:

Parametric form of the practical stability limit:

$$\left[ P_p^2 + (Q_p - Q_0)^2 \right]^2 - \left[ P_p^2 + (Q_p - Q_0)^2 \right] \cdot \left[ (4as)^2 + 2a(Q_p - Q_0) \right] + a^2(Q_p - Q_0)^2 = 0. \quad (30)$$

Praktična granica stabilnosti prikazana je na slici 1 krivuljom F.

Practical stability limit is represented by curve F in Figure 1.



#### 4.6 Ograničenje rada generatora zbog zagrijavanja čeonog prostora

Neki generatori osjetljivi su na trajni rad u poduzbudi i u dijelu stabilnog rada zbog povećanog lokalnog zagrijavanja magnetski i električki vodljivih dijelova stroja u čeonom prostoru. Iskustva pokazuju da je ograničenje kod starijih generatora zbog te pojave strože od granice praktične granice stabilnosti [13].

Poznato je da najveće vrijednosti rezultirajuće indukcije u čeonom prostoru nastaju u kompenzatorskom režimu poduzbude, a najmanje u kompenzatorskom režimu naduzbude. Fizikalno je to tumačeno činjenicom da se pri induktivnoj struji statora protjecanja rotora i armature odmažu, a pri kapacitivnoj struji potpomažu. Pri tome je utjecajniiji armaturni namot, jer je smješten bliže paketu statora. U naduzbuđenom radu statorsko polje je oslabljeno djelovanjem uzbuđenog protjecanja.

##### 4.6.1 Fizikalno objašnjenje magnetskih pojava u čeonom dijelu sinkronog stroja

Pod utjecajem protjecanja uzbuđenog i armaturnog namota čeonu prostor sinkronog stroja se ispunjava magnetskim poljem koje, u određenoj kombinaciji ovih protjecanja, može rezultirati dovoljno velikom uzdužnom komponentom magnetske indukcije u paketu statora (zubima i jarmu), da izazove dodatna lokalna zagrijavanja, najčešće u zubima i u području oko korijena zuba, opasna po izolaciju među limovima, te opasna po izolaciju vodiča na mjestima izlaska iz utora [14] i [15].

Ulančeno protjecanje uzbuđenog namota i namota armature stvara magnetski napon zračnog raspora onog iznosa, koji je potreban za stvaranje glavnog magnetskog toka potrebnog za induciranje napona namota statora, nužnog za elektromehaničku pretvorbu. Magnetski napon zračnog raspora stvara u čeonom prostoru stroja magnetsko polje čiju raspodjelu prikazuje slika 4 (izabran je slučaj praznog hoda, kako bi se što jasnije ocrtale magnetske silnice stvorene samo magnetskim naponom zračnog raspora, tj. bez rasipnog magnetskog polja namota armature).

Protjecanje armaturnog namota stvara rasipno polje u čeonom prostoru sinkronog stroja, što prikazuje slika 5.

Zajedničko djelovanje oba protjecanja je prikazano na slici 6 rezultatnim poljem, i to:

- za slučaj induktivnog opterećenja stroja,  $\varphi_{\text{ind}} = 0$  (slika 6a),

#### 4.6 Limitation of generator operation on account of the end region heating

Some generators are sensitive to constant operation in the underexcitation mode and in part of the steady operation on account of the rising local heating of magnetically and electrically conductive parts of the machine in the end region. Experience has shown that the limitation in older generators on this account is stricter than the practical stability limit [13].

It is known that the biggest values of the resulting induction in the end region occur in the underexcitation compensating mode, and the smallest in the overexcitation compensating mode. Physically, this has been ascribed to the fact that the rotor flux and the armature flux are hindering in case of the inductive stator current, and that they are helping in case of the capacitive current. In this the armature winding has the greater effect, because it is located closer to the stator package. In the overexcited operation the stator field is weakened by the effect of the excitation flux.

##### 4.6.1 Physical explanation of the magnetic occurrences in the end region of the synchronous machine

Under the influence of the flux in the excitation and the armature windings, the end region of the synchronous machine is filled with the magnetic field which, in a certain combination of these fluxes, may result in sufficiently sized longitudinal component of the magnetic induction in the stator package (teeth and yoke) to cause additional local heating, most often in the teeth and in the area around teeth roots, which is dangerous to the insulation between sheet-metal strips and for the insulation of the conductors where they emerge from the slots [14] and [15].

The chain flux of the excitation winding and the armature winding creates magnetic voltage in the air gap with the value needed to create the main magnetic flux that is required for inducing the stator winding voltage, which is necessary for the electromechanical transformation. The magnetic voltage of the air gap creates a magnetic field in the end region of the machine whose distribution is shown in Figure 4 (no-load case has been selected to enable the magnetic lines, which are created by the magnetic voltage of the air gap, i.e. without the magnetic stray field of the armature winding, to stand out as clearly as possible).

The flux of the armature winding creates a stray field in the end region of the synchronous machine, as shown in Figure 5.

The combined effect of both fluxes is presented by means of the resultant field in Figure 6:

- za slučaj kapacitivnog opterećenja stroja,  $\cos \varphi_{\text{cap}} = 0$  (slika 6b).

Pri induktivnom opterećenju rasipno polje, stvoreno protjecanjem namota armature, u čeonom prostoru ima suprotan smjer djelovanja u uzdužnom pravcu u odnosu na polje koje stvara magnetski napon zračnog raspora. Stoga je rezultirajuća aksijalna komponenta indukcije u čeonom prostoru bitno manja od one koju stvara kapacitivno opterećenje stroja.

Pri kapacitivnom opterećenju se slika polja bitno mijenja. Rasipno polje namota armature u čeonom prostoru ima isti smjer djelovanja u uzdužnom pravcu u odnosu na polje koje stvara magnetski napon zračnog raspora. Dakle, u čeonom prostoru pri kapacitivnom opterećenju dolazi do povećanja ukupne aksijalne komponente indukcije, što može dovesti do njenog opasnog povećanja; specifični gubici u krajnjim limovima paketa statora, u koje magnetski tok ulazi okomito na njihovu površinu [16] i [17], su mnogostruko veći od gubitaka pri toku koji ulazi u lim uzdužno. Kako su gubici vrtložnih struja proporcionalni kvadratu indukcije, to i pri manjim indukcijama mogu nastati opasna lokalna zagrijavanja, a s tim u vezi i problemi koji su već prije iskazani:

- visoka lokalna temperatura koja znatno ubrzava starenje izolacije između limova,
- ostarjela izolacija između limova se mrvlji i dijelom nestaje, što omogućava povećanje amplitude vibracija zubiju, s konačnom posljedicom: lom zuba uslijed umora materijala, njegovo ispadanje, što može (vrlo vjerojatno) dovesti do mehaničkih oštećenja izolacije namota, a time i do teških kvarova,
- dodatno zagrijavanje izolacije namota koja je u neposrednom kontaktu s pregrijanim limovima, što također dovodi do ubrzanog lokalnog starenja izolacije i time stvaranja uvjeta za proboj.

- at the inductive machine load,  $\cos \varphi_{\text{ind}} = 0$  (Figure 6a),
- at the capacitive machine load,  $\cos \varphi_{\text{cap}} = 0$  (Figure 6b).

At the inductive load the stray field, created by the flux of the armature winding, shows the opposite longitudinal direction in the end region compared with the field created by the magnetic voltage of the air gap. The resulting axial component of the induction in the end region is substantially smaller than the one created by the capacitive machine load.

At the capacitive load the picture of the field changes considerably. The stray field of the armature winding in the end region has the same longitudinal direction compared with the field created by the magnetic voltage of the air gap. Consequently, at the capacitive load the end region experiences a higher total axial component of the induction, which may lead to its dangerous increase; the specific losses in the end sheet-metal strips of the stator package, which the magnetic flux enters perpendicularly to their plane [16] and [17], are many times greater than the losses when the flux enters the sheet-metal strips longitudinally. Since eddy current losses are proportionate to the induction square, even lower induction may cause dangerous local heating and the related problems that have already been mentioned:

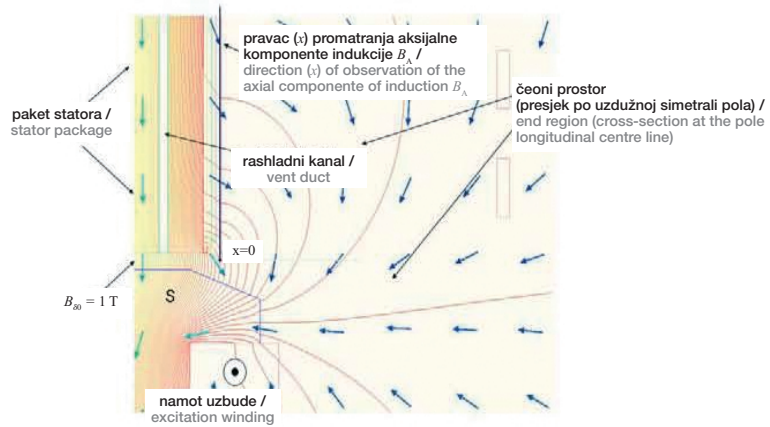
- high local temperature, considerably speeding the ageing of the insulation between sheet-metal strips,
- old insulation between sheet-metal strips crumbles and partly vanishes, which enables higher amplitude of teeth vibration, finally resulting in a tooth broken on account of fatigue, and its falling out, with the (very probable) possibility of mechanical damage to the insulation of the winding, which spells out severe breakdowns,
- additional heating of the winding insulation in direct contact with overheated sheet-metal strips, which also leads to faster local ageing of the insulation and creating conditions for a breach.

**Slika 4**

Magnetske prilike u  
čeonom prostoru za  
slučaj praznog hoda

**Figure 4**

Magnetic conditions  
in the end region at  
no-load

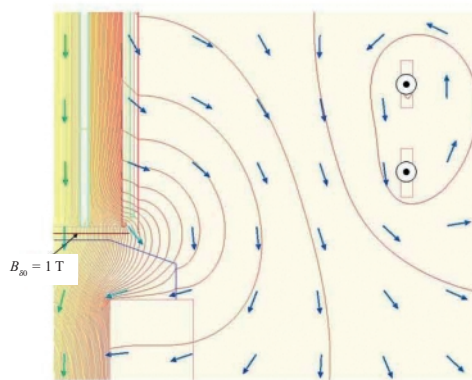


**Slika 5**

Magnetske prilike u  
čeonom prostoru stvorene  
protjecanjem namota  
armature

**Figure 5**

Magnetic conditions in  
the end region created by  
the flux of the armature  
winding

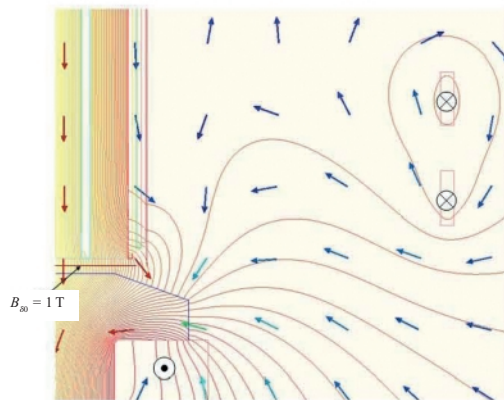


**Slika 6**

Magnetske prilike u  
čeonom prostoru stvorene  
kombiniranim djelovanjem  
magnetskog napona  
zračnog raspóra i rasipnog  
polja statorskog namota

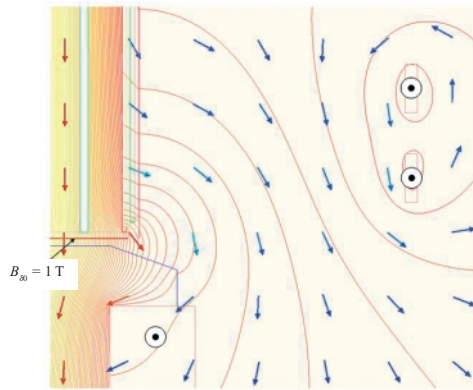
**Figure 6**

Magnetic conditions in  
the end region created by  
the combined effect of the  
magnetic voltage of the air  
gap and the stray field of  
the stator winding

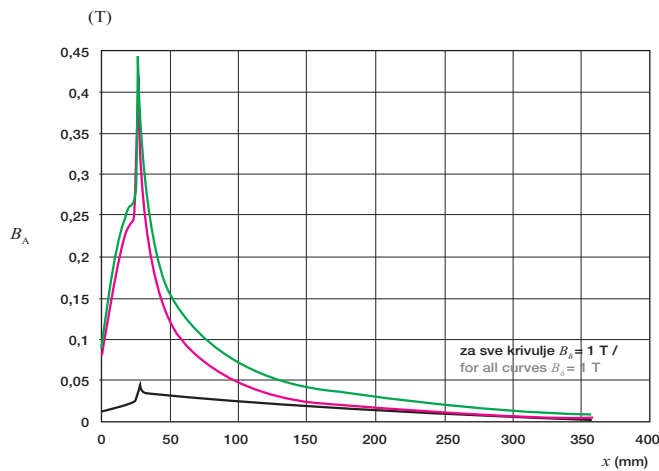


a) Magnetske prilike u čeonom prostoru za slučaj induktivnog opterećenja / Magnetic conditions in the end region at the inductive load

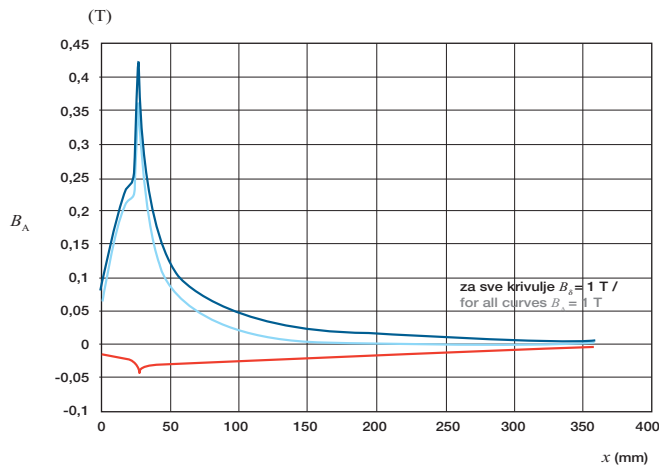




b) Magnetske prilike u čeonom prostoru za slučaj kapacitivnog opterećenja / Magnetic conditions in the end region at the capacitive load



a) za kapacitivno opterećenje / for the capacitive load



b) za induktivno opterećenje / for the inductive load

### Slika 7

Dijagram raspodjele (dobivene proračunom) uzdužne komponente indukcije  $B_A$  u krajnjem limu paketa statora u čeonom prostoru hidrogeneratora HE Vinodol (vidi pravac promatranja na slici 4)

### Figure 7

Distribution diagram (obtained by calculation) of the longitudinal component of induction  $B_A$  in the end sheet-metal strip of the stator package in the end region of the hydrogenerator of HPP Vinodol (see the direction of observation in Figure 4)

- Raspodjela  $B_A$  u praznom prostoru pri  $B_\delta = 1 \text{ T}$  / Distribution of  $B_A$  in the empty space at  $B_\delta = 1 \text{ T}$
- Raspodjela  $B_A$  (samo od rasipnog polja struje armature), kapacitivni teret,  $I_m \cos \varphi = 0$  / Distribution  $B_A$  (from the stray field of the armature current only), capacitive load,  $I_m \cos \varphi = 0$
- Raspodjela  $B_A$  pri  $I_m \cos \varphi = 0$  cap (kapacitivno),  $B_\delta = 1 \text{ T}$  / Distribution  $B_A$  at  $I_m \cos \varphi = 0$  cap (capacitive),  $B_\delta = 1 \text{ T}$

- Raspodjela  $B_A$  u praznom prostoru pri  $B_\delta = 1 \text{ T}$  / Distribution of  $B_A$  in the empty space at  $B_\delta = 1 \text{ T}$
- Raspodjela  $B_A$  (samo od rasipnog polja struje armature), induktivni teret,  $I_m \cos \varphi = 0$  ind / Distribution  $B_A$  (from the stray field of the armature current only), inductive load,  $I_m \cos \varphi = 0$
- Raspodjela  $B_A$  pri  $I_m \cos \varphi = 0$  ind (induktivno),  $B_\delta = 1 \text{ T}$  / Distribution  $B_A$  at  $I_m \cos \varphi = 0$  ind (inductive),  $B_\delta = 1 \text{ T}$

Slika 7, dobivena numeričkim proračunom (uz pomoć MKE) raspodjele magnetskog polja za konkretan generator (hidroagregat broj 3 u HE Vinodol), prikazuje raspodjelu aksijalne komponente indukcije uz paket statora u simetrali pola, u radialnom smjeru od zračnog raspora pa do vanjskog ruba paketa. Raspodjela polja, koja odgovara ovoj slici, prikazana je na slikama 4, 5 i 6.

#### 4.6.2 Određivanje aksijalne komponente magnetskog polja pomoću fazorskog dijagrama

Elektromagnetske prilike u čeonom prostoru se mogu opisati fazorskim dijagramima na način sličan onome na koji se opisuju naponske i strujne prilike u aktivnom dijelu sinkronog generatora (SG). Nužno je pretpostaviti linearne odnose, tj. treba zanemariti zasićenje u čeonom dijelu: polne papuče pola, zuba i jarma statora. U slučajevima u kojima ovaj način proračuna ukaže na visoke iznose indukcije, mogu se mjerenjima, i/ili točnijim proračunima uz pomoć metode konačnih elemenata, provjeriti stvarne elektromagnetske prilike čeonog prostora.

Fizikalne veličine (i njihove p.u. vrijednosti), koje su bitne u opisu elektromagnetskih prilika čeonog prostora naznačenog na slikama 4 do 7, jesu:

- $U_n$  – nazivni napon (radi utvrđivanja veličine magnetskog napona zračnog raspora u PH),
- $E$  – EMS za bilo koje pogonsko stanje (radi utvrđivanja veličine magnetskog napona zračnog raspora za bilo koje pogonsko stanje),
- $X_{2\sigma}$  ( $x_{2\sigma}$ ) – rasipna reaktancija (radi utvrđivanja veličine magnetskog napona zračnog raspora za bilo koje pogonsko stanje, tj. za izračun  $E$ ),
- $I_a$  ( $i_a = I_a / I_{an}$ ) – struja armature (p.u.),
- $B_{A\delta n}$  ( $b_{A\delta n} = B_{A\delta n} / B_{A\delta n} = 1$ ) – aksijalna (uzdužna) komponenta magnetske indukcije u čeonom prostoru sinkronog generatora za PH pri  $U_n$  (mag. indukcija koju uzrokuje samo magnetski napon zračnog raspora u praznom hodu, tj. pri  $E = U_n$ ),
- $B_{A\sigma n}$  ( $b_{A\sigma n} = B_{A\sigma n} / B_{A\delta n}$ ) – aksijalna (uzdužna) komponenta magnetske indukcije u simetrali protjecanja namota armature sinkronog generatora, koju uzrokuje samo rasipno polje namota armature pri  $I_{an}$ ,
- $B_{An}$  ( $b_{An} = B_{An} / B_{A\delta n}$ ) – aksijalna (uzdužna) rezultirajuća komponenta magnetske indukcije u čeonom prostoru, uzrokovana djelovanjem magnetskog napona zračnog raspora i rasipnog polja namota armature, pri  $I_{an}$  i pri  $U_n$  sinkronog generatora,
- $B_{A\delta}$  ( $b_{A\delta} = B_{A\delta} / B_{A\delta n} = i_a b_{A\delta n}$ ) – aksijalna (uzdužna) komponenta magnetske indukcije u simetrali rezultirajućeg protjecanja sinkronog generatora, uzrokovana magnetskim naponom

Figure 7, a result of the numerical calculation (with the support of the FEM) of the distribution of the magnetic field for a specific generator (Unit 3 at HEPP Vinodol), shows the distribution of the axial component of the induction at the stator package in the pole centre line, in the radial direction from the air gap to the outer edge of the package. The field distribution corresponding to this figure is shown in Figures 4, 5 and 6.

#### 4.6.2 Determining the axial component of the magnetic field by means of the phasor diagram

Electromagnetic conditions in the end region can be described by means of the phasor diagrams in the manner similar to the description of the voltage and current conditions in the active part of the synchronous generator (SG). It is necessary to assume linear relations, i.e. the saturation in the end region is to be neglected: pole tabs of poles, teeth and yoke of the stator. In the cases in which this type of calculation indicates higher induction values, the actual electromagnetic conditions in the end region can be checked by measurement and/or more accurate calculations with the help of the finite element method.

The physical values (and their p.u. values) which are relevant to the description of the electromagnetic conditions in the end region shown in Figures 4 to 7 are:

- $U_n$  – the rated voltage (to determine the value of the magnetic voltage of the air gap in PH),
- $E$  – electromagnetic force for any operating status (to determine the value of the magnetic voltage of the air gap for any operating status),
- $X_{2\sigma}$  ( $x_{2\sigma}$ ) – stray reactance (to determine the value of the magnetic voltage of the air gap for any operating status, i.e. for the calculation of  $E$ ),
- $I_a$  ( $i_a = I_a / I_{an}$ ) – the armature current (p.u.),
- $B_{A\delta n}$  ( $b_{A\delta n} = B_{A\delta n} / B_{A\delta n} = 1$ ) – the axial (longitudinal) component of the magnetic induction in the end region of the synchronous generator for PH at  $U_n$  (mag. induction caused by the magnetic voltage of the air gap at no load, i.e. at  $E = U_n$ ),
- $B_{A\sigma n}$  ( $b_{A\sigma n} = B_{A\sigma n} / B_{A\delta n}$ ) – the axial (longitudinal) component of the magnetic induction at the centre line of the armature winding flux of the synchronous generator, caused by the stray field of the armature winding at  $I_{an}$ ,
- $B_{An}$  ( $b_{An} = B_{An} / B_{A\delta n}$ ) – the axial (longitudinal) resulting component of the magnetic induction in the end region, caused by the effect of the magnetic voltage of the air gap and the armature winding stray field, at  $I_{an}$  and  $U_n$  of the synchronous generator,

zračnog raspora pri bilo kojoj struji armature, bilo kojem  $\cos \varphi$  i odgovarajućoj struji uzbude, ali uz  $U_n$ ,

- $B_{A\sigma}$  ( $b_{A\sigma} = B_{A\sigma} / B_{A\delta n} = i_a b_{A\sigma n}$ ) – aksijalna (uzdužna) komponenta magnetske indukcije u simetrali protjecanja namota armature sinkronog generatora, koju uzrokuje samo rasipno polje namota armature pri bilo kojoj struji armature, bilo kojem  $\cos \varphi$ ,
- $B_A$  ( $b_A = B_A / B_{A\delta n} = i_a b_{An}$ ) – aksijalna (uzdužna) rezultirajuća komponenta magnetske indukcije u čeonom prostoru, uzrokovana djelovanjem magnetskog napona zračnog raspora i rasipnog polja namota armature, za bilo koju radnu točku sinkronog generatora pri  $U_n$ .

Proračunom (kontinuirano kao na slici 7), i/ili mjerenjem (točkasto u skladu s postavljenim Hall-ovim sondama), možemo bez većih poteškoća odrediti  $B_{A\delta n}$  u praznom hodu, a zatim  $B_{A\sigma n}$  ili/  $B_{An}$ . Poznavajući ove veličine, možemo za bilo koje pogonsko stanje, i za bilo koju točku na izabranoj osi prema slici 4 odnosno 7 (os  $x$ ), u radijalnom smjeru od zračnog raspora pa do vanjskog ruba paketa, odrediti veličinu  $B_A$ .

Vektorski dijagrami indukcija u čeonom prostoru, za karakteristična pogonska stanja, prikazani su na slici 9 a), b), c) i d). Prikaz na ovoj slici je izveden iz odgovarajućeg dijagrama na slici 8.

Iz dijagrama na slici 9 slijedi jednostavna računica za određivanje rezultirajuće aksijalne komponente indukcije u čeonom prostoru:

- a) i b) za induktivna opterećenja,  $\varphi > 0$ :

$$b_A = \sqrt{(b_{A\sigma} - i_a x_\sigma)^2 + 1 - 2(b_{A\sigma} - i_a x_\sigma) \cos\left(\frac{\pi}{2} - \varphi\right)}, \quad (31)$$

$$b_A = \sqrt{(b_{A\sigma\sigma} - x_\sigma)^2 i_a^2 + 1 - 2(b_{A\sigma\sigma} - x_\sigma) i_a \sin \varphi}, \quad (32)$$

$$b_A = \sqrt{(b_{A\sigma\sigma}^2 - 2b_{A\sigma\sigma} x_\sigma + x_\sigma^2) i_a^2 + 1 - 2(b_{A\sigma\sigma} - x_\sigma) i_a \sin \varphi}, \quad (33)$$

- $B_{A\delta}$  ( $b_{A\delta} = B_{A\delta} / B_{A\delta n} = i_a b_{A\delta n}$ ) – the axial (longitudinal) component of the magnetic induction at the centre line of the resulting flux of the synchronous generator, caused by the magnetic voltage of the air gap at any armature current, any  $\cos \varphi$  and the corresponding excitation current, but at  $U_n$ ,

- $B_{A\sigma}$  ( $b_{A\sigma} = B_{A\sigma} / B_{A\delta n} = i_a b_{A\sigma n}$ ) – the axial (longitudinal) component of the magnetic induction at the centre line of the armature winding flux of the synchronous generator, caused by the stray field of the armature winding at any armature current, any  $\cos \varphi$ ,

- $B_A$  ( $b_A = B_A / B_{A\delta n} = i_a b_{An}$ ) – the axial (longitudinal) resulting component of the magnetic induction in the end region, caused by the effect of the magnetic voltage of the air gap and the stray field of the armature winding, for any operating point of the synchronous generator at  $U_n$ .

By calculation (continuously as in Figure 7) and/or by measurement (spot measurement following the installed Hall probes) we can without greater difficulties determine  $B_{A\delta n}$  at no load, then  $B_{A\sigma n}$  or/ and  $B_{An}$ . Knowing these values, we may determine the value of  $B_A$  for any operating condition and any point on the selected axis as shown in Figure 4 and 7 ( $x$  axis), in the radial direction from the air gap to the outer edge of the package.

The vector diagrams of the induction in the end region, for characteristic operating statuses, are shown in Figures 9 a), b), c) and d). The presentation in this figure has been derived from the appropriate diagram in Figure 8.

From the diagram in Figure 9 follows the simple calculation for determining the resulting axial component of the induction in the end region:

- a) and b) for the inductive load,  $\varphi > 0$ :

– c) i d) za kapacitivno opterećenje,  $\varphi < 0$ :

$$b_A = \sqrt{(b_{A\sigma} - i_a x_\sigma)^2 + 1 - 2(b_{A\sigma} - i_a x_\sigma) \cos\left(\frac{\pi}{2} + \varphi\right)}, \quad (34)$$

$$b_A = \sqrt{(b_{A\sigma\sigma} - x_\sigma)^2 i_a^2 + 1 + 2(b_{A\sigma\sigma} - x_\sigma) i_a \sin \varphi}, \quad (35)$$

$$b_A = \sqrt{(b_{A\sigma\sigma}^2 - 2b_{A\sigma\sigma} x_\sigma + x_\sigma^2) i_a^2 + 1 + 2(b_{A\sigma\sigma} - x_\sigma) i_a \sin \varphi}. \quad (36)$$

Korištenjem Microsoft Excel-a može se jednostavnim programom napisane relacije koristiti za izračun nepoznate fizikalne veličine.

Proračun primjenom metode konačnih elemenata daje raspodjelu  $B_{A\delta n}$  i  $B_{A\sigma n}$  po osima njihovog protjecanja. Ako pretpostavimo da je magnetska vodljivost čeonog prostora neovisna o položaju osi protjecanja (uzbudnog namota, namota armature, rezultirajućeg protjecanja), što gotovo u potpunosti vrijedi za turbo izvedbe, dok kod izraženih polova postoje odstupanja, to se obradom dobivenih raspodjela, prema gore provedenoj računici, mogu relativno jednostavno dobiti veličine i raspodjele rezultirajuće indukcije u čeonom prostoru sinkronog generatora.

Ukoliko se želi u pogonski dijagram uključiti prikaz aksijalne komponente magnetske indukcije za bilo koje pogonsko stanje, tj. za bilo koju radnu točku, može se na kružnicu pogonskog dijagrama dodati kružnica ovisnosti rezultirajuće magnetske indukcije  $B_A$  (odnosno  $b_A$ ) izrazom koji slijedi iz fazorskog dijagrama na slici 9. Jednadžba kružnice (hodograma) glasi:

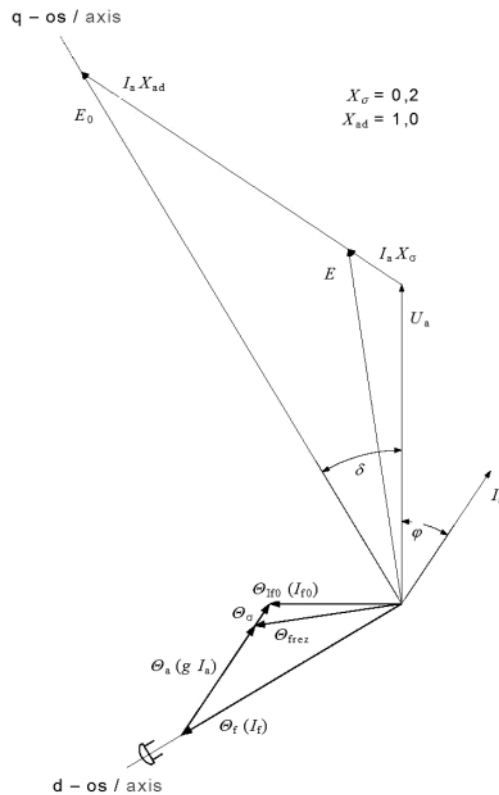
$$y^2 + (x + b_{A\delta\delta})^2 = (b_{A\sigma\sigma} - x_\sigma)^2. \quad (37)$$

– c) and d) for the capacitive load,  $\varphi < 0$ :

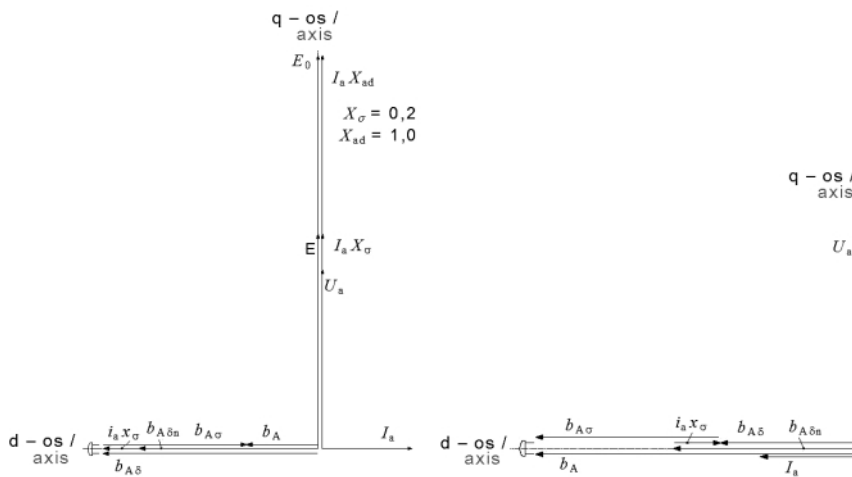
By using Microsoft Excel it is possible, by means of a simple program, to use the relations written for the calculation of an unknown physical value.

The calculation by using the finite element method gives the distribution of  $B_{A\delta n}$  and  $B_{A\sigma n}$  on their flux axes. If we assume that the magnetic conductivity of the end region is independent of the position of the flux axis (of the excitation winding, the armature winding, the resulting flux) - which almost entirely applies to turbo designs, whereas in pronounced poles there are deviations - processing the distributions obtained, according to the above-mentioned calculation, it is easy to obtain the values and distributions of the resulting induction in the end region of the synchronous generator.

If one wants to include in the PQ diagram a presentation of the axial component of the magnetic induction for any operating status, i.e. for any operating point, it is possible to add on the circle of the PQ diagram the circle of the dependence of the resulting magnetic induction  $B_A$  (i.e.  $b_A$ ) by means of the expression derived from the phasor diagram in Figure 9. The equation of the circle (flowchart) reads:



**Slika 8**  
 Vektorsko-fazorski dijagram SG kao temelj za izradu odgovarajućeg dijagrama odnosa protjecanja i indukcija u čeonom prostoru generatora  
 Figure 8  
 Vector-phasor diagram SG as the basis for preparing the corresponding relation diagram for the flux and induction in the end region of the generator

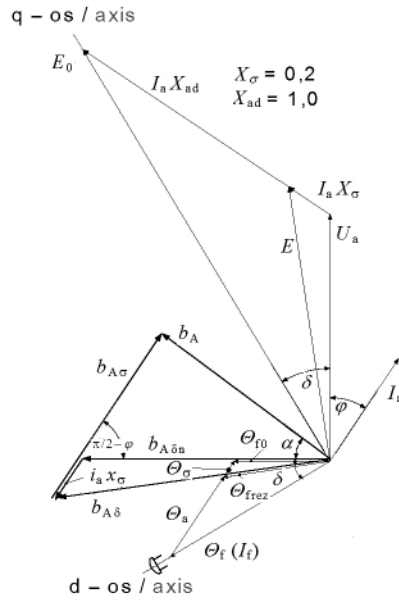


a) pri  $\cos \varphi = 0$  induktivno / at  $\cos \varphi = 0$  inductive

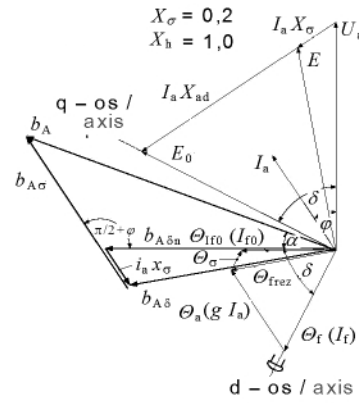
c) pri  $\cos \varphi = 0$  kapacitivno / at  $\cos \varphi = 0$  capacitive

**Slika 9**  
 Vektorsko-fazorski dijagrami za indukcije u čeonom prostoru SG za karakteristična pogonska stanja  
 Figure 9  
 Vector-phasor diagrams for inductions in SG end region for characteristic operating conditions





b) za bilo koje induktivno opterećenje / for any inductive load



d) za bilo koje kapacitivno opterećenje / for any capacitive load

Na slici 10 prikazan je hodogram indukcije u jednoj točki čeonog prostora u ovisnosti o faktoru snage uz konstantnu struju armature.

Figure 10 shows induction flowchart in one point of the end region dependent on the power factor at the constant armature current.

Radijus kružnice na slici 10 može se odrediti prema izrazu:

The radius of the circle in Figure 10 may be determined according to the expression:

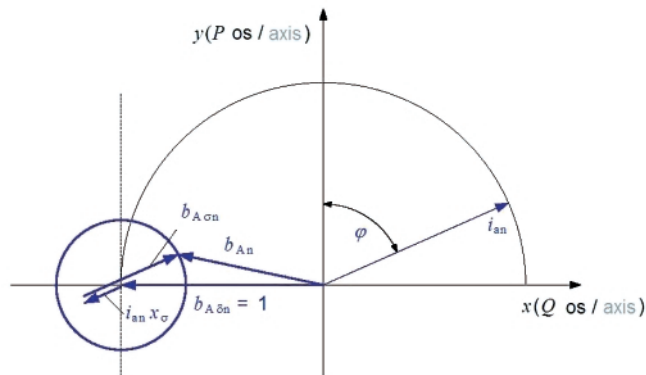
$$r_A = b_{A\sigma n} - x_{2\sigma} \cdot \quad (38)$$

**Slika 10**

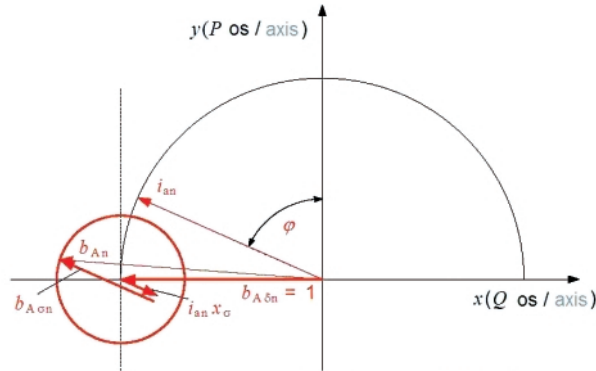
Hodogram indukcije u jednoj točki čeonog prostora u ovisnosti o faktoru snage uz konstantnu struju armature

**Figure 10**

Flowchart of the induction at one point of the end region dependent on the power factor at the constant armature current



a) za induktivno opterećenje / for the inductive load



b) za kapacitivno opterećenje / for the capacitive load

#### 4.6.3 Granica dozvoljenog zagrijavanja čeonog prostora

U slučaju da su provediva mjerenja uzdužne komponente magnetske indukcije  $B_A$ , kuta opterećenja  $\delta$ , pripadnih veličina za  $\cos \varphi$ , struja i napona uzbude i armature, može se, na temelju iskustvenih relacija iz literature [18], [19] i [20] odrediti granica dozvoljenog zagrijavanja u čeonom prostoru sinkronog stroja.

Ta granica može se predočiti dijelom kružnice čiji radijus iznosi:

$$R_T = k_{\text{topl}} \cdot U^2 \cdot k_c, \quad (39)$$

a središte se nalazi na osi  $x$  na udaljenosti  $q_0$  od ishodišta:

$$q_0 = \frac{U^2 \cdot k_A \cdot k_c}{1 - k_A}, \quad (40)$$

gdje su:

- $k_{\text{topl}}$  – koeficijent zagrijavanja,
- $k_c$  – kratkospojni omjer generatora  $k_c = I_{f0} / I_{fk}$ ,
- $k_A$  – koeficijent koji govori o utjecaju uzbuđenog protjecanja na aksijalnu komponentu magnetskog polja za promatrano mjesto u čeonom prostoru,
- $U$  – linijski napon na stezaljkama generatora.

Parametar  $k_A$  određuje se tako, da se za nekoliko radnih točaka snime indukcija  $B_A$ , kut opterećenja  $\delta$ , faktor snage  $\varphi$ , te struje i naponi armature i uzbude.

#### 4.6.3 Limit of permitted end region heating

In case of executable measurements of the longitudinal component of the magnetic induction  $B_A$ , load angle  $\delta$ , corresponding values of  $\cos \varphi$ , excitation and armature current and voltage, it is possible, on the basis of referenced experience relations [18], [19] and [20], to determine the limit of the permitted heating in the end region of the synchronous machine.

This limit can be presented as part of the circle whose radius is:

and its centre is at axis  $x$  at distance  $q_0$  from the originating point:

whereas:

- $k_{\text{topl}}$  – heating coefficient,
- $k_c$  – short-circuit ratio of the generator  $k_c = I_{f0} / I_{fk}$ ,
- $k_A$  – coefficient indicating the effect of the excitation flux on the axial component of the magnetic field for the observed location in the end region,
- $U$  – line voltage on generator clamps.

Parameter  $k_A$  is determined so that for several operating points induction  $B_A$ , load angle  $\delta$ , power factor  $\varphi$ , and the armature and excitation currents and voltages are recorded.

Prema fazorskom dijagramu na slici 11, vrijedi da je  $\sigma = 1 - k_A$ . Iznosi za  $\sigma$  i  $k_2$  se kreću između 0 i 1. Iz istog dijagrama dobije se izraz za koeficijent  $k_2$ :

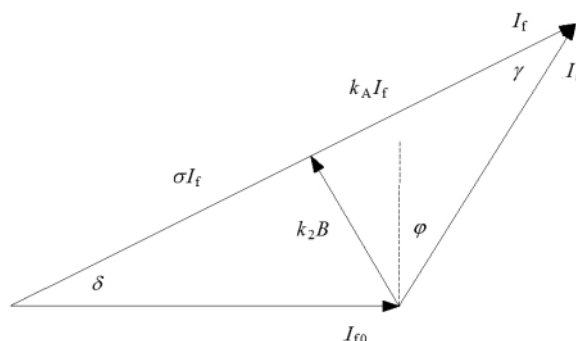
$$k_2 = \frac{\sqrt{(\sigma I_f)^2 + I_{f0}^2 - 2\sigma I_f I_{f0} \cos \delta}}{B}, \quad (41)$$

a koji je pomoćna varijabla pri određivanju koeficijenta  $k_A$ .

According to the phasor diagram in Figure 11, it notes that  $\sigma = 1 - k_A$ . The values for  $\sigma$  and  $k_2$  are between 0 and 1. From the same diagram we obtain the expression for coefficient  $k_2$ :

which is an auxiliary variable in determining coefficient  $k_A$ .

**Slika 11**  
Fazorski dijagram za naduzbuđeno stanje generatora u kojem su prikazani koeficijenti  $\sigma$  i  $k_A$   
**Figure 11**  
Phasor diagram for overexcited generator status, showing coefficients  $\sigma$  and  $k_A$



Odabere se nekoliko radnih točaka za koje su provedena snimanja na generatoru. Za svaku tu radnu točku uzima se iznos parametra  $\sigma$  između 0 i 1 u što finijim koracima, te se za svaku radnu točku i određeni  $\sigma$  računaju odstupanja parametra  $k_2$  od njegove srednje vrijednosti. Odabere se onaj  $\sigma$  za koji je odstupanje paramtera  $k_2$  za odabrane radne točke najmanje.

Nakon što je opisanim postupkom dobiven parametar  $\sigma$ , moguće je odrediti i parametar  $k_A$  kao:

$$k_A = 1 - \sigma. \quad (42)$$

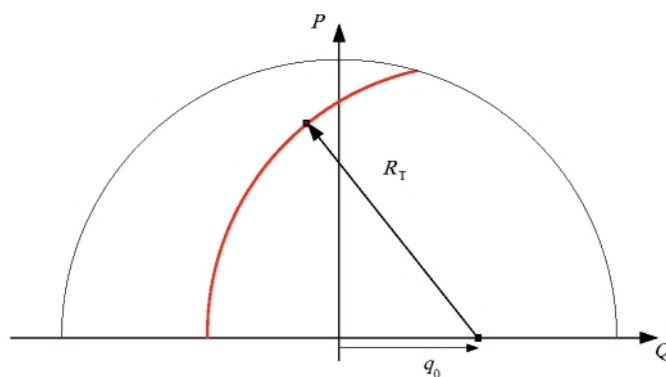
Nakon što je poznat i parametar  $k_A$ , moguće je odrediti položaj središta kružnice (40).

Several operating points are selected for which recordings on the generator are made. For each operating point the value of parameter  $\sigma$  ranges between 0 and 1 in the finest increments possible, and for each operating point and specific  $\sigma$ , the deviations of parameter  $k_2$  from its mean value are calculated. One selects  $\sigma$  for which the deviation of parameter  $k_2$  for the selected operating points is the smallest.

Once the procedure described has delivered parameter  $\sigma$ , it is possible to determine  $k_A$  as:

When parameter  $k_A$  is known, too, it is possible to determine the position of the centre of the circle (40).

**Slika 12**  
 Granica zagrijavanja  
 čeonog prostora  
**Figure 12**  
 Thermal limit in the end  
 region



Da bi se odredio radijus kružnice potrebno je iz snimljenih radnih točaka pokusom zagrijavanja odrediti radnu točku u kojoj je postignuto maksimalno dopušteno zagrijavanje u čeonom prostoru, a koje je određeno propisima. To je jedna od točaka (slika 12) kroz koju prolazi kružnica ograničenja zagrijavanja čeonog prostora. Udaljenost te točke od centra kružnice određenog prema (40) predstavlja polumjer  $R_T$  (39) pa je moguće odrediti i koeficijent  $k_{topl}$ .

#### 4.7 Ograničenje rada generatora zbog minimalnog i maksimalnog napona armature generatora

Jedan od bitnih parametara generatora, koji se može naći na natpisnoj pločici generatora, je nazivni napon i njegovo dopušteno odstupanje. Uobičajeno odstupanje napona kreće se od 5 % do 10 % nazivne vrijednosti [21].

Regulacijski sustav generatora najčešće održava nazivnu vrijednost napona na stezaljkama generatora uz zadanu statiku po kompenzaciji jalove struje. Jalova snaga, te zbog toga i faktor snage s kojim radi generator na mreži, ovise o naponu na stezaljkama generatora, definiranoj djelatnoj snazi koju generator daje u mrežu, kratkospojnoj reaktanciji transformatora i naponu mreže u čvorištu priljučka transformatora.

Slika 13 prikazuje fazorski dijagram pomoću kojeg se prikazuju fazno-amplitudni odnosi između napona mreže i napona generatora. U dijagramu su pomoćnim kružnicama ucrtane vrijednosti minimalnog i maksimalnog napona na stezaljkama generatora. Minimalni i maksimalni napon u per unit sustavu mreže računaju se prema sljedećim izrazima:

In order to determine the radius of the circle it is necessary to determine, on the basis of the operating points recorded and by test heating, the operating point with the maximum permitted heating in the end region, as defined by regulations. It is one of the points (Figure 12) through which the circle of the thermal limit in the end region passes. The distance of this point from the centre of the circle determined in accordance with (40) is radius  $R_T$  (39), making it possible to also define coefficient  $k_{topl}$ .

#### 4.7 Limitation of generator operation on account of the minimum and maximum armature voltages

One of the relevant parameters of the generator, which can be found in the nameplate of the generator, is the rated voltage and its permitted tolerance. The usual tolerance for the voltage ranges from 5 % to 10 % of the rating [21].

The regulation system of the generator mostly maintains the rated voltage value on the clamps, at a determined static for the compensation of the reactive current. Reactive power, and consequently the power factor of the generator on the network, depend on the voltage on the clamps, the defined active power delivered by the generator to the network, the short-circuit reactance of the transformer, and the voltage of the network at the transformer connection node.

Figure 13 shows the phasor diagram used to present phase-amplitude relations between the network voltage and the generator voltage. On the auxiliary circles of the diagram the values of the minimum and maximum voltages on the clamps are entered. The minimum and the maximum voltages in a per unit network system are calculated in accordance with the following expressions:

$$u_{g\text{mmax}} = u_{g\text{max}} \cdot U_{gn} \cdot \frac{U_{t2n}}{U_{t1n}} \cdot \frac{1}{U_{mn}}, \quad (43)$$

$$u_{g\text{mmin}} = u_{g\text{min}} \cdot U_{gn} \cdot \frac{U_{t2n}}{U_{t1n}} \cdot \frac{1}{U_{mn}}, \quad (44)$$

gdje su:

$U_{t1n}$  – nazivni napon primara blok-transformatora,  
 $U_{t2n}$  – nazivni napon sekundara blok-transformatora.

Uz ispunjenu pretpostavku  $U_{gn} = U_{t1n}$  ovi izrazi se mogu pojednostavniti:

whereas:

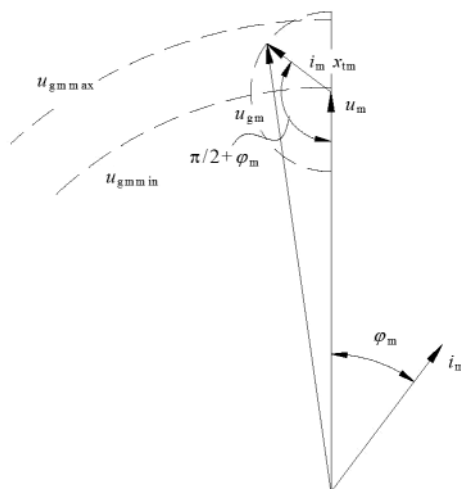
$U_{t1n}$  – rated voltage of the block transformer primary,  
 $U_{t2n}$  – rated voltage of the block transformer secondary.

Under the assumption  $U_{gn} = U_{t1n}$  these expressions can be simplified:

$$u_{g\text{mmax}} = u_{g\text{max}} \cdot \frac{U_{t2n}}{U_{mn}}, \quad (45)$$

$$u_{g\text{mmin}} = u_{g\text{min}} \cdot \frac{U_{t2n}}{U_{mn}}. \quad (46)$$

**Slika 13**  
 Fazorski dijagram  
 generatora i blok-  
 transformatora na mreži  
 Figure 13  
 Phasor diagram of the  
 generator and the block  
 transformer on the  
 network



Ostale oznake na slici 13 su:

$i_m$  – struja generatora preračunata na stranu mreže,  
 $x_{lm}$  – kratkospojna reaktancija blok transformatora,  
 $u_m$  – napon mreže,  
 $\varphi_m$  – faktor snage na strani mreže.

Množenjem fazora na slici 13 s  $u_{mn}/x_{lm}$ , te zakretanjem za  $\pi/2$ , dobiva se pogonski dijagram sinkronog agregata zajedno s blok-transformatorom, gledan sa strane mreže. Prethodno ucrtane granice minimalnog i maksimalnog napona postaju granice u dijagramu snage određene dozvoljenim

Other markings in Figure 13:

$i_m$  – generator current calculated on the network side,  
 $x_{lm}$  – short-circuit reactance of the block transformer,  
 $u_m$  – network voltage,  
 $\varphi_m$  – power factor on the network side.

By multiplying the phasor in Figure 13 by  $u_{mn}/x_{lm}$ , and turning by  $\pi/2$ , we obtain the PQ diagram of the synchronous unit with the block transformer, as seen from the network side. The previously entered limits of the minimum and maximum voltages become the limits in the power diagram determined



maksimalnim i minimalnim iznosima napona generatora (slika 14).

Povećanje napona, ovisno o faktoru snage i iznosu opterećenja može voditi nedozvoljenom povećanju uzbuđne struje, ali to je ograničenje zasebno određeno.

Smanjeni napon generatora utječe na njegovu sposobnost stabilnog rada u poduzbuđenom stanju. Kao i u slučaju povišenog napona, i ovo ograničenje posebno je definirano granicom stabilnog rada generatora (agregata).

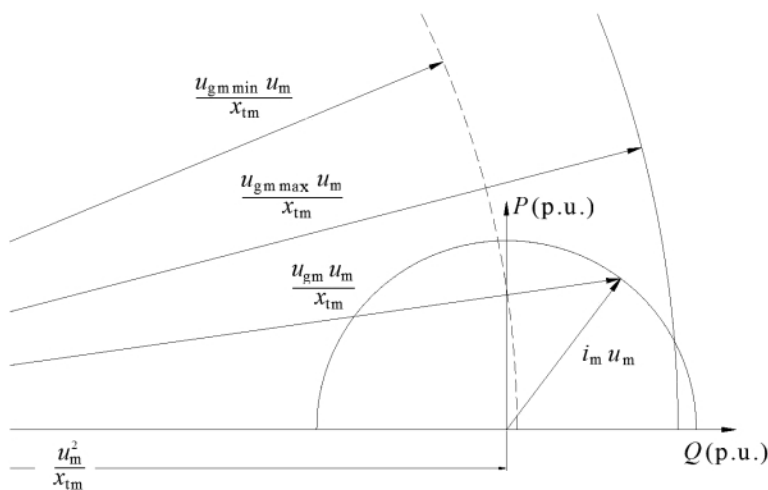
Ograničenja nastala zbog minimalnog i maksimalnog radnog napona generatora prikazana na slici 14 različito su postavljena u odnosu na pogonsku kartu za sva tri napona mreže (nazivni, povišeni i sniženi) za koje se crta pogonska karta agregata s blok-transformatorom. No, ta ograničenja u pravilu nisu u stvarnosti aktualna (osim u slučaju da postoji izrazita nelogičnost u dopuštenim povišenim ili sniženim naponima mreže i generatora). Naime, generator neće nikada raditi kapacitivno opterećen, ako je napon mreže snižen, odnosno generator neće raditi izrazito induktivno opterećen, ako je napon mreže povišen.

by the permitted maximum and minimum values of the generator voltages (Figure 14).

Higher voltage, depending on the power factor and the load, may lead to a non-permitted increase in the excitation current, but this limitation is determined separately.

Lower generator voltage affects its capability of stable operation in the underexcited state. As with higher voltage, this limitation, too, is separately defined by the stable operation limit of the generator (unit).

The limitations occurring on account of the minimum and maximum operating voltages of the generator as shown in Figure 14 are positioned differently with regard to the PQ diagram for all three network voltages (rated, higher, and lower) for which the PQ diagram of the unit with the block transformer is drawn. However, these limitations, as a rule, do not count in reality (unless there is a pronounced lack of logic in the permitted higher or lower voltages of the network and the generator). Notably, the generator will never operate capacitatively loaded if the network voltage is lower, i.e. the generator will not operate inductively loaded if the network voltage is higher.



**Slika 14**  
Fazorski dijagram generatora i blok-transformatora na mreži, granice minimalnog i maksimalnog napona generatora  
Figure 14  
Phasor diagram of the generator and the block transformer on the network, the limits of the minimum and maximum generator voltages

## 5 POKUSI POTREBNI ZA ODREĐIVANJE PARAMETARA KLJUČNIH PRI ODREĐIVANJU POGONSKE KARTE

### 5.1 Algoritam metodologije dobivanja korisničke pogonske karte

Pokusi potrebni za određivanje parametara KPK, a samim time i za crtanje KPK, određeni su metodologijom određivanja pogonske karte sinkronog hidroagregata. Ta metodologija, uključivo s blok-transformatorom, može se najjednostavnije prikazati blok dijagramom na slici 15. Pogonska karta se može odrediti na tri razine:

- informativna, samo na temelju proračuna,
- informativna, na temelju proračuna i mjerenja bez ugradnji dodatnih senzora,
- stvarna, na temelju proračuna i mjerenja s dodatno ugrađenim sensorima.

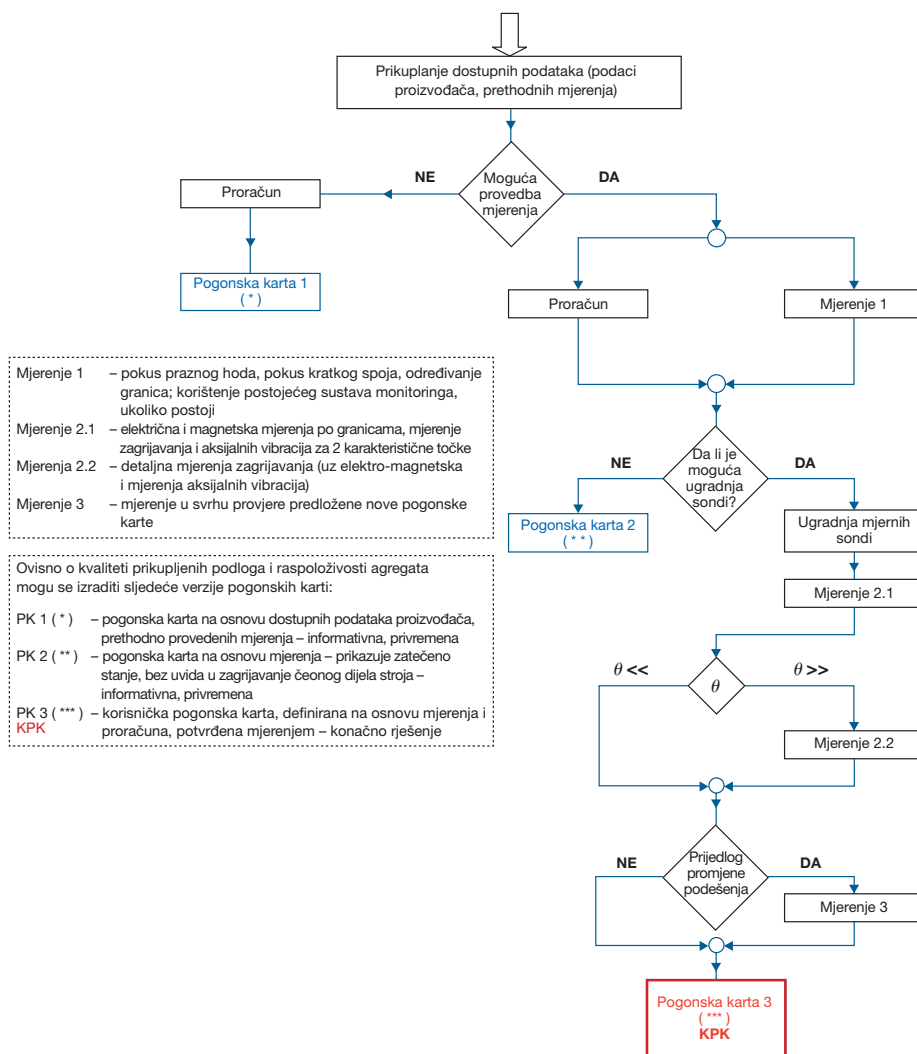
## 5 TESTS NECESSARY TO DETERMINE KEY PARAMETERS IN DETERMINING PQ DIAGRAM

### 5.1 Algorithm of the methodology to obtain the actual PQ diagram

The tests necessary to determine the APQ parameters, and consequently to draw the APQ, are determined by the methodology to determine the PQ diagram of the synchronous turbine-generator unit. This methodology, including the block transformer, can most simply be presented in a flowchart in Figure 15. The PQ diagram may be determined on three levels:

- indicative, on the basis of calculation only,
- indicative, on the basis of calculation and measurements without installing additional sensors,
- real, on the basis of calculation and measurements with additionally installed sensors.

**Slika 15**  
Dijagram toka metodologije za određivanje KPK (korisničke pogonske karte) sinkronog agregata, uključivo s blok-transformatorom  
**Figure 15**  
Flowchart of the methodology to determine APQ (actual PQ diagram) of the synchronous unit, including the block transformer

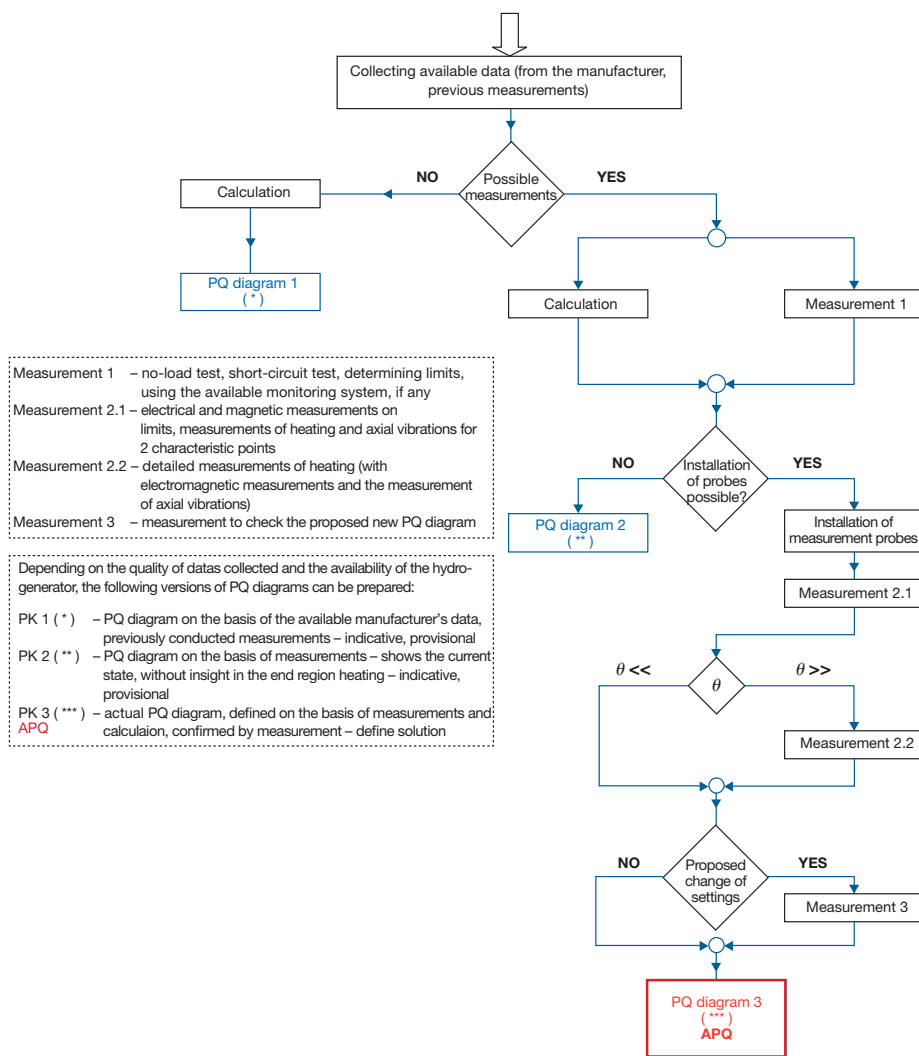


Informativne pogonske karte na prvoj razini (a) ni u kom slučaju ne daju sigurne granice, a tek je nešto bolja situacija s informativnom pogonskom kartom druge razine (b). Tek stvarna pogonska karta (c), potvrđena mjerenjem, omogućava siguran rad hidroagregata s točno definiranim ograničenjima, i time predstavlja konačan cilj istraživanja kao KORISNIČKA POGONSKA KARTA (KPK).

Realna je situacija za hidroagregate u HEP-u takva da će se stvarna pogonska karta (KPK) u većini hidroagregata pokazati manje restriktivna od trenutno postavljenih ograničenja. Korekcijom limita, koji bi se postavili po stvarnim pogonskim kartama svih hidroagregata, valja očekivati elastičnije ponašanje hidroagregata u nestandardnim stanjima EES s obzirom na potrebe jalove snage u mreži.

The indicative PQ diagram on the first level (a) does not by any means provide reliable limits, and the situation is only slightly better with the indicative PQ diagram on the second level (b). Only the real PQ diagram (c), confirmed by measurement, enables safe operation of the hydrogenerator with accurately defined limitations, and represents the ultimate goal of the research – the ACTUAL PQ DIAGRAM (APQ).

The real status of the hydrogenerators of HEP will lead to the actual PQ diagrams (APQ) of most hydrogenerators proving less restrictive than the limitations currently in force. Following the correction of the limits to be set on the basis of the actual PQ diagrams of all the hydrogenerators, more flexible behaviour of hydrogenerators should be expected in non-standard states of the power generation system with regard to the reactive power requirements of the network.



Dobivanje stvarne korisničke pogonske karte (KPK) sinkronog agregata, uključivo s blok-transformatorom, uvjetovano je, dakle, ugradnjom dodatnih senzora u čeonu prostor generatora, nakon čega slijede mjerenja aksijalne komponente magnetskog polja i temperatura na ključnim mjestima. Ugradnja mjernih sonde zahtijeva detaljno poznavanje konstrukcije stroja i specifičnosti ventilacijskog sustava, te odabir primjerene tehnologije ugradnje.

Odabrane su sljedeće pozicije za ugradnju sonde:

- dvije pozicije na krajnjem statorskom limu, jedna na rubu do provrta i druga na 1/3 visine zuba od ruba provrta,
- jedna pozicija na tlačnom prstu do ruba, na mjestu što bližem provrtu,
- jedna pozicija na tlačnoj ploči do ruba, na mjestu što bližem provrtu.

Ako postoji opravdana sumnja o nestandardnoj asimetričnoj ventilaciji po obodu u čeonom prostoru, potrebno je ugraditi dodatne temperaturne sonde simetrično po obodu na krajnjem limu na još barem 3 mjesta (ili drugačije postavljenim ako sustav ventilacije to nalaže, tj. ako postoje blokirana područja za protok rashladnog zraka). Te sonde treba smjestiti na približno  $\frac{1}{2}$  visine zuba.

Kratkotrajna mjerenja čine mjerenja sljedećih veličina za minimalno 10 radnih točaka:

- struja armature, 3 fazne veličine,
- napon generatora, 3 veličine (fazne ili linijske),
- faktor snage, 3 fazne veličine,
- djelatna snaga (ili se računa iz rezultata mjerenja struje, napona i faktora snage),
- jalova snaga (ili se računa iz rezultata mjerenja struje, napona i faktora snage),
- struja uzbude (ili uzbude uzбудnika ako je uzbuda nedostupna),
- napon uzbude (ili uzbude uzбудnika ako je uzbuda nedostupna),
- kut opterećenja  $\delta$ ,
- indukcije (signali sa svih Hallovih sonde),
- temperature (signali sa svih termo-sonde),
- ostale veličine koje su mjerljive ugrađenim strujnim i naponskim transformatorima,
- signali s ostalih ugrađenih senzora, kao npr. vibracije, temperature, protoci rashladnog medija, magnetsko polje u rasporu, duljina zračnog raspora itd.,
- napon mreže, 3 veličine (fazne ili linijske).

Obtaining the actual PQ diagram (APQ) for the synchronous unit, including the block transformer, depends on the installation of additional sensors in the end region of the generator, followed by the measurements of the axial component of the magnetic field and temperatures in key locations. The installation of measurement probes requires detailed knowledge of the design of the machine and the specific characteristics of the ventilation system, as well as the selection of the appropriate installation technology.

The following positions have been selected for the installation of probes:

- two positions on stator end sheet-metal strips, one on the edge of the bore and the other at 1/3 height of the tooth from the edge of the bore,
- one position on the pressure finger on the edge, at the closest possible location to the bore,
- one position on the pressure plate on the edge, at the closest possible location to the bore.

If there is reason to suspect a non-standard asymmetrical ventilation along the rim in the end region, it is necessary to install additional thermal probes symmetrically along the rim on the end sheet-metal strips at min. 3 more places (or distributed otherwise if the ventilation system requires it, i.e. in case there are areas blocking the passage of cooling air). These probes should be placed approximately at  $\frac{1}{2}$  of the tooth height.

Short measurements include the measurements of the following characteristics for a minimum of 10 operating points:

- armature current, 3 phase values,
- generator voltage, 3 values (phase or line),
- power factor, 3 phase values,
- real power (or calculated from the results of the measurements of the current, voltage and power factor),
- reactive power (or calculated from the results of the measurements of the current, voltage and power factor),
- excitation current (or the excitation of the exciter if the excitation is not available),
- excitation voltage (or the excitation of the exciter if the excitation is not available),
- load angle  $\delta$ ,
- inductions (signals from all the hall probes),
- temperature (signals from all the thermal probes),
- other characteristics measurable by means of installed current and voltage transformers,
- signals from other installed sensors, e.g. vibrations, temperatures, coolant flows, magnetic field in the air gap, length of the air gap etc.,
- network voltage, 3 values (phase or line).

Tablica 1 – Popis radnih točaka za mjerenja zagrijavanja  
Table 1 – List of operating points to measure heating

Oznaka / Designation	$P$	$Q$	Opis / Description
T01	0	0	prazni hod / no-load
T02	0	$-Q_{\max}, P = 0$	čisto kapacitivni teret / purely capacitive load
T03	0	$+Q_{\max}, P = 0$	čisto induktivni teret / purely inductive load
T04	$P_n/3$	$-Q_{\max}, P = P_n/3$	djelomični djelatno-kapacitivni teret / partly active-capacitive load
T05	$P_n/3$	$+Q_{\max}, P = P_n/3$	djelomični djelatno-induktivni teret / partly active-inductive load
T06	$P_n/2$	$-Q_{\max}, P = P_n/2$	djelomični djelatno-kapacitivni teret / partly active-capacitive load
T07	$P_n/2$	$+Q_{\max}, P = P_n/2$	djelomični djelatno-induktivni teret / partly active-inductive load
T08	$2P_n/3$	$-Q_{\max}, P = 2P_n/3$	djelomični djelatno-kapacitivni teret / partly active-capacitive load
T09	$2P_n/3$	$+Q_{\max}, P = 2P_n/3$	djelomični djelatno-induktivni teret / partly active-inductive load
T10	$P_n$	$-Q_{\max}, P = P_n$	puni djelatno-kapacitivni teret / full active-capacitive load
T11	$P_n$	0	puni djelatni teret / full active load
T12	$P_n$	$+Q_{\max}, P = P_n$	puni djelatno-induktivni teret / full active-inductive load

Ako se mjerenja obavljaju za minimalni broj radnih točaka, to trebaju biti sljedeće radne točke prikazane u tablici 1: T01, T02, T03, T04, T05, T08, T09, T10, T11, T12.

Ako je definirana minimalna djelatna snaga za trajni rad, tada točke T04 i T05 treba snimati pri toj minimalnoj djelatnoj snazi.

Sva mjerenja treba obaviti uz konstantan napon generatora (što je na nekim elektranama u pravilu teško izvedivo), a u protivnom poželjno je ista mjerenja ponoviti u različito doba dana (tako da se ostvari snimanje cijelog seta mjerenja s različitim naponima), kako bi preračunavanje na nazivni napon bilo korektnije obavljeno.

Analizom rezultata navedenih mjerenja utvrđuju se predvidivi problemi za promatrani hidrogenerator, te obavljaju dugotrajna mjerenja za minimalno 6 radnih točaka, pri čemu se mjere i temperature

If the measurements are conducted for the minimum number of operating points, the following operating points are needed as represented in Table 1: T01, T02, T03, T04, T05, T08, T09, T10, T11, T12.

If the minimum active power for constant operation is defined, points T04 and T05 need to be recorded at that minimum active power.

All the measurements need to be conducted at constant generator voltage (which, as a rule, is difficult to achieve in some power plants), otherwise they should be repeated at different times during the day (so that the entire measurement set with different voltages is applied), in order to do the recomputation for the rated voltage as accurately as possible.

By analysing the results of these measurements the foreseeable problems of the observed hydrogenerator are determined and long-lasting measurements for a minimum of 6 points are conducted, including the



uz pomoć dodatno ugrađenih sondi. Na temelju prethodnih mjerenja može se približno predvidjeti na kojim temperaturama će se zagrijavanje ustaliti, pa treba prvih nekoliko sati raditi s povećanim zagrijavanjem, tako, da se proces zagrijavanja ubrza do približno stacionarne temperature. Preporuča se dugotrajna mjerenja obaviti za sljedeće radne točke prikazane u tablici 1: T02, T03, T06, T07, T10, T12.

Analizom rezultata proračuna i dugotrajnih mjerenja konačno se utvrđuju koeficijenti pomoću kojih se ucrta granica zagrijavanja čeonog prostora.

Sustavima za daljinsko beskontaktno mjerenje, koji se u zadnje vrijeme pojavljuju u uporabi, otvara se dodatna mogućnost za idealnim određivanjem granice zagrijavanja rotora u 1. kvadrantu pogonske karte. Tako bi mjerenjima na ključnim najtoplijim mjestima na rotoru tu granicu valjalo utvrditi kao stvarnu termičku granicu, koja nije ovisna samo o uzbudnoj struji. Zato se preporuča ugrađivanje takvog sustava (barem u nove i revitalizirane hidrogeneratore) kojim bi se granica zagrijavanja rotora definirala dopuštenom temperaturom, a ne dopuštenom uzbudnom strujom. Kako do sada nisu ugrađeni beskontaktni sustavi za mjerenje više veličina s rotora, u ovom članku se samo predlaže dorada idealne granice u nadzubi čim se ti mjerni uvjeti ostvare. Za sada je granica u nadzubi definirana klasičnim načinom, dakle maksimalno dopuštenom uzbudnom strujom.

S obzirom na relativno bitno jeftiniji način utvrđivanja elektromagnetskih stanja i parametara sinkronog generatora, treba sustavno uhodavati i primjenjivati metodu konačnih elemenata (MKE) za sve one pojave i parametre za koje je ova metoda prikladna. Provedena istraživanja na agregatu broj 3 HE Vinodol, a dijelom i na TE Plomin, ukazuju na nužno povezivanje mjerenja i proračuna pri određivanju stanja fizikalnih veličina i parametara sinkronog stroja pri postavljanju KPK.

## 5.2 Pokusi praznog hoda i kratkog spoja

Da bi se odredila struja  $I_{10}$  potrebno je snimiti pokus praznog hoda generatora u koracima od 15-ak točaka. Za iznos nazivnog napona generatora  $U_n$  očita se iznos struje  $I_{10}$ . Na snimljenoj karakteristici  $U = f(I_p)$  provuče se pravac kroz ishodište, a koji predstavlja karakteristiku praznog hoda nezasićenog generatora. S tog pravca se za nazivni napon  $U_n$  očita iznos struje  $I_{10}$ .

Za određivanje iznosa struje  $I_{1k}$  potrebno je snimiti pokus kratkog spoja generatora. Iz krivulje ovisnosti  $I = f(I_p)$  za struju  $I_n$  očita se struja  $I_{1k}$ .

measurement of temperatures by means of the additionally installed probes. On the basis of the measurements conducted it can be approximately predicted at which temperatures the heating will become steady, consequently in the first few hours it is necessary to operate with increased heating so that the heating process is speeded up to the approximately stationary temperature. It is recommendable to conduct long-lasting measurements for the following operating points shown in Table 1: T02, T03, T06, T07, T10, T12.

By analysing the results of the calculation, long-lasting measurement coefficients are definitely determined by means of which the thermal limit of the end region is then plotted.

With systems for remote contactless measurement, which are being increasingly used recently, there is the additional possibility for an ideal determination of the rotor heating limit in quadrant 1 of the PQ diagram. Measurements on the key hotspots on the rotor should determine this limit as the real thermal limit which is not dependent solely on the excitation current. It is, therefore, recommendable to install such a system (at least in new and remanufactured hydrogenerators) to define the rotor thermal limit in terms of the temperature permitted, not the permitted excitation current. Contactless systems for measuring multiple values on the rotor have not been installed yet, so this paper only suggests supplemental treatment of the ideal overexcitation limit when such measurement conditions are provided. Presently, the overexcitation limit is defined in the traditional way, that is by the maximum permitted excitation current.

Considering the much cheaper method for determining electromagnetic states and parameters of a synchronous generator, the finite element method (FEM) should be systematically introduced and used for all the occurrences and parameters where this method is appropriate. The research conducted at Unit 3 of HPP Vinodol, and partly at TPP Plomin, points to the necessity to link measurements to the calculation for determining the status of physical values and parameters of the synchronous machine in establishing the APQ.

## 5.2 No-load and short-circuit tests

In order to determine current  $I_{10}$  it is necessary to record the generator no-load test in increments of about 15 points. As the value of rated generator voltage  $U_n$ , the reading of current value  $I_{10}$  is taken. On recorded characteristic  $U = f(I_p)$  a line is drawn through the originating point to represent the no-load characteristic of the non-saturated generator. From this line the reading of current value  $I_{10}$  is taken as the rated voltage  $U_n$ .

Iz karakteristika pokusa praznog hoda i kratkog spoja mogu se odrediti relativna vrijednost nezasićene reaktancije generatora  $X_d$  kao i kratkospojni omjer  $k_c$ :

$$X_d = \frac{I_{fk}}{I_{fg}}, \quad (47)$$

$$k_c = \frac{1}{\frac{I_{fk}}{I_{f0}}}. \quad (48)$$

### 5.3 Određivanje rasipne reaktancije

U svrhu određivanja rasipne reaktancije sinkronog stroja potrebno je na sredinu zuba statorskog paketa, najmanje 10 cm udaljeno od ruba paketa, ugraditi Hallove sonde, kako bi se na tom mjestu omogućilo mjerenje indukcije pri pokusima kratkog spoja i praznog hoda.

Indukcija  $B_{phn}$ , izmjerena pri nominalnom naponu na stezaljkama generatora u praznom hodu, predstavlja mjeru magnetiziranja stroja za 100 % napona armature.

Indukcija  $B_{ksn}$ , izmjerena pri pokusu kratkog spoja uz nominalnu struju armature, predstavlja mjeru magnetiziranja stroja u kratkom spoju za 100 % struje armature; ova je indukcija nužna za induciranje EMS-a što ga traži rasipni pad napona armaturnog namota.

Veličina rasipne reaktancije – relativna vrijednost – se, iz opisanih mjerenja u pokusima praznog hoda i kratkog spoja, dobiva kao omjer indukcija u kratkom spoju i praznom hodu:

$$X_{2\sigma} = \frac{B_{ksn}}{B_{phn}}, \quad (49)$$

ili u postotnim vrijednostima:

$$X_{2\sigma\%} = 100 \cdot \frac{B_{ksn}}{B_{phn}}. \quad (50)$$

Metoda, koja je upravo opisana, omogućuje određivanje rasipne reaktancije koja je bitno točnija

To determine current value  $I_{fk}$  it is necessary to record the short-circuit test of the generator. From dependence curve  $I = f(I_f)$  the reading of current  $I_{fk}$  is taken for current  $I_n$ .

From the characteristics of the no-load and short-circuit tests, the relative value of non-saturated reactance of generator  $X_d$  and short-circuit ratio  $k_c$  can be determined:

### 5.3 Determining stray reactance

In order to determine the stray reactance of the synchronous machine it is necessary to install Hall probes in the middle of a tooth in the stator package, at least 10 cm away from the edge of the package, to enable the measurement of the induction in short-circuit and no-load tests.

Induction  $B_{phn}$ , measured at the rated voltage on the generator clamps in the no-load mode, represents the measure of machine magnetization at 100 % of the armature voltage.

Induction  $B_{ksn}$ , measured in the short-circuit test at the rated armature current, represents the measure of machine short-circuit magnetization at 100 % of the armature current; this induction is necessary for inducing the electromagnetic force required by the stray voltage drop in the armature winding.

The (relative) value of the stray reactance is obtained from the described measurements during no-load and short-circuit tests as a ratio of short-circuit and no-load inductions:

or as percentage (%) values:

The described method makes it possible to determine the stray reactance with much more accuracy

u odnosu na računom dobivene vrijednosti, jer se određuje u gotovo istim magnetskim stanjima zasićenosti rasipnih putova u željezu kao u slučaju nominalnog pogonskog opterećenja stroja.

#### 5.4 Pokus zagrijavanja u čeonom prostoru generatora

Mjerenja zagrijavanja čeonog dijela stroja, tijekom kojih se pored električnih i temperaturnih veličina, očitavaju i indukcije u čeonom prostoru, spadaju u vremenski zahtjevnije pokuse provedene na sinkronom generatoru. Svaka radna točka mjeri se u trajanju od nekoliko sati, kako bi se ustalile mjerene temperature. Svrha mjerenja temperatura u čeonom prostoru je provjera stvarnih mogućnosti rada u kapacitivnom području rada generatora s obzirom na lokalno dodatno zagrijavanje krajnjih limova i ostalih dijelova u čeonom prostoru generatora.

Za potrebe ovih mjerenja u generator se postavljaju termosonde za mjerenje temperatura čeonog dijela generatora kao i Hallove sonde koje mjere pripadne indukcije. Raspored termo i Hallovih sondi, koje je potrebno ugraditi u generator, određen je u 5.1.

Pokus se provodi tako da generator u odabranoj radnoj točki radi trajno sve dok se temperatura izabranih točaka u tijeku jednog sata ne mijenja više od 0,5 °C.

Potrebno je za daljnji izračun uzeti minimalno tri radne točke (preporuča se i više). Odabire se rezultat mjerenja one sonde u čeonom prostoru koja je izmjerila najveću temperatura na kraju pokusa zagrijavanja.

than the calculated values, because it is determined in almost all the magnetic states of the saturation of stray routes in iron, as in the case of the rated operating load of the machine.

#### 5.4 Heating test in the generator end region

Measurements of the heating in the end region of the machine, during which readings of inductions in the end region of the machine are made in addition to the reading of electrical and temperature values, belong to more demanding tests conducted on the synchronous generator in terms of duration. Each operating point is measured for several hours in order to steady the temperatures measured. The purpose of measuring the temperatures in the end region is to check the actual performance in the capacitive area of generator operation considering the local additional heating of the end sheet-metal strips and other parts in the end region of the generator.

To conduct these measurements thermal probes are placed in the generator to measure the temperatures in the end region of the generator, as well as Hall probes to measure the related inductions. The distribution of the thermal and Hall probes in the generator is determined in 5.1.

The test is conducted so as to have the generator operate constantly in the selected operating point as long as the temperature of the selected points does not change by more than 0.5 °C within one hour.

For further calculation it is necessary to take at least three operating points (even more is recommendable). The measuring result of the probe with the highest recorded temperature at the end of the heating test in the end region is selected.

## 6 ZAKLJUČAK

Korisnička pogonska karta neophodan je dokument za svaku proizvodnu jedinicu električne energije. Od podjednake je važnosti osoblju u elektrani i operatoru prijenosnog sustava.

Dobro poznavanje mogućnosti proizvodnih jedinica od vitalne je važnosti, kako iz tehničkog gledišta, tako i ekonomskog, posebno u uvjetima tržišnog natjecanja.

Određivanje korisničke pogonske karte potrebno je provesti jer se time mogu otkriti neiskorišteni potencijali generatora ili se pak usporedbom s prethodnim rezultatima mogu primijetiti promjene koje mogu na vrijeme ukazati na probleme. Pojedine granice korisničke pogonske karte starenjem generatora podložne su izmjenama, te je njihova provjera i osvježavanje poželjno.

Međutim, osim unošenja klasičnih granica kao okvira u kojima se smiju nalaziti pogonske točke sinkronog generatora, potrebno je posvetiti pažnju još nekim mogućnostima prikaza ponašanja proizvodne jedinice unutar sebe i prema prijenosnoj mreži. Naime, nedavno provedena istraživanja za potrebe HEP-a su pokazala da tvorbu korisničke pogonske karte (KPK) treba proširiti s dvije dopune. S jedne strane treba provjeriti elektromagnetska, a s tim u vezi i toplinska stanja u čeonom prostoru generatora, dok s druge strane treba proširiti KPK na način da se u nju uključi i blok-transformator. Time se dobiva KPK sinkronog agregata kao cjelovite energetske proizvodne (pretvaračke) jedinice priključene na stezaljke prijenosne mreže.

Elektromagnetska stanja u čeonom prostoru hidrogeneratora (kod nekih tipova s obzirom na konstrukciju i elektromagnetska opterećenja) mogu dovesti do dodatnih, lokalno vrlo intenzivnih, gubitaka, a s tim u vezi i do povećanja zagrijavanja. Ova pojava je posebno izražena u slučajevima rada duboko u kapacitivnom, tj. drugom kvadrantu KPK. Budući da mogu nastupiti kritična lokalna pregrijanja dinamo limova u čeonom dijelu paketa statora, koja pri duljem vremenskom trajanju uništavaju, mrve izolaciju između limova, to, uslijed trajno prisutnih vibracija, može doći do otpadanja zubiju zbog zamora materijala, a time i do nepredvidivih, ali vrlo vjerojatno teških posljedica mehaničkog oštećenja visokonaponske izolacije vodiča i glava namota.

Kontrola elektromagnetskih prilika u čeonom prostoru sinkronog generatora se, u pravilu, provodi na dva načina, mjerenjem (uzdužne komponente magnetske indukcije, te istovremeno

## 6 CONCLUSION

The actual PQ diagram is a necessary document for any electric power generation unit. It is of equal importance for the power plant staff and for the transmission system operator.

Good knowledge of the performance capabilities of power generation units is vital both technically and economically, particularly under the conditions of market competition.

It is necessary to determine the actual PQ diagram because it may reveal unused potentials of the generator, or a comparison with previous results may reveal changes that could indicate problems just in time. Some limits in the actual PQ diagram are subject to changes as the generator ages, and their checks and updates are desirable.

However, apart from entering the most common limits as a framework within which the operating points of the synchronous generator may be positioned, it is necessary to pay due attention to some other possibilities for the presentation of the behaviour of the power generation unit within itself and towards the transmission network. Recent research conducted on behalf of HEP has shown that the creation of the actual PQ diagram (APQ) needs to be extended by two additions. On the one hand it is necessary to check the electromagnetic and, in the same context, the thermal conditions in the end region of the generator, whereas on the other hand it is necessary to extend the APQ by including the block transformer. This will produce the APQ of the synchronous power generator as an integral power generating (conversion) unit connected to the clamps of the transmission network.

Electromagnetic states in the end region of the hydrogenerator (in some types considering the design and electromagnetic loads) may lead to additional, locally very intensive losses and consequent rising heating. This occurrence is particularly noticeable during the operation deep within the capacitive, i.e. the second quadrant of the APQ. Since there may occur critical local overheating of the dynamo sheet-metal strips in the end region of the stator package, which over time destroys, crumbles the insulation between the sheets, there is a possibility, due to permanent vibrations, for the teeth to fall off because of fatigue, which may lead to unforeseeable, but very probably severe effects of the mechanical damage to the high-voltage insulation of conductors and winding heads.

The control of electromagnetic conditions in the end region of the synchronous generator is generally

i temperature zuba i korijena zubiju krajnjih limova paketa statora) i/ili proračunima (uz pomoć metode konačnih elemenata).

Osim kontrole elektromagnetskih i toplinskih prilika, poželjna je i kontrola vibracija glava namota i krajnjih limova paketa statora, posebno kod većih proizvodnih jedinica.

Vizualizacijom korisničke pogonske karte na način da se sve granice dopuštenog rada sinkronog agregata prikažu na ekranu prikladne veličine i oštrote prikaza, kako bi se u svakom trenutku pogona mogla pratiti pogonska dinamika vizualnim praćenjem položaja pogonske točke u i izvan okvira dopuštenih granica, dobila bi se bitno veća brzina upravljanja, a povećala sigurnost rada pojedinih proizvodnih jedinica u okvirima pripadnog elektroenergetskog sustava.

conducted in two ways: by measurement (of the longitudinal component of magnetic induction, and simultaneously the temperature of the tooth and roots of the teeth of end sheet-metal strips of the stator package), and/or by calculation (with the help of the finite element method).

In addition to the control of the electromagnetic and thermal conditions, it is desirable to control the vibrations of the winding heads and end sheet-metal strips of the stator package, particularly in bigger generating units.

The visualisation of the actual PQ diagram – to the effect that all the limits of the permitted operation of the synchronous unit are displayed on the screen of an appropriate size and resolution, to make it possible to monitor, at any time during the operation, the operational dynamics by visually checking the position of the operating point within and beyond the permitted limits – would bring a much quicker responsiveness in managing the units, and it would improve the operating safety of individual power generation units within the respective power supply system.



---

## LITERATURA / REFERENCES

- [1] MALJKOVIĆ, Z., Mogućnosti rada sinkronih generatora u poduzbuđenom stanju, CIGRE okrugli stol: Naponske prilike u mreži 400 kV i stabilnost EES-a, Cavtat, 2002.
- [2] MARUŠIĆ, A., Zaštita od smetnji u elektroenergetskom sustavu, CIGRE okrugli stol: Naponske prilike u mreži 400 kV i stabilnost EES-a, Cavtat, 2002.
- [3] HIRVONEN, R., et al., Is There Market for Reactive Power Services – Possibilities and Problems, Proceedings of the CIGRE, group 39, R.39-213, Paris, 2000
- [4] SIROTIĆ, Z., MALJKOVIĆ, Z., Sinkroni strojevi, skripta, Zagreb, 1996.
- [5] POŽAR, H., Proizvodnja električne energije - 1 dio, Svezak 2, skripta, Zagreb, 1978.
- [6] ZLATANOVIĆ, D. et al., Determination of the Actual PQ Diagram of the Hydrogenerators, Being in Service, in Order to Establish Their Maximum Operating Domains and Their Capacity to Provide System Services, Proceedings of the CIGRE, group A1, R.A1-203., Paris, 2004
- [7] ERCEG, G., et al., Excitation Limiters for Small Synchronous Generators, 11<sup>th</sup> EDPE, October, 2000
- [8] IEEE Task Force on Excitation Limiters, Underexcitation Limiter Models for Power System Stability Studies, IEEE Transaction on Energy Conversion, Vol. 10, No. 3, September 1995
- [9] ROGER BERUBE, G., et al., A Utility Perspective on Under-Excitation Limiters, IEEE Transaction on Energy Conversion, Vol. 10, No. 3, September, 1995
- [10] GIRGIS, G. K., VU, H.D., Verification of Limiter Performance in Modern Excitation Control Systems, IEEE Transaction on Energy Conversion, Vol. 10, No. 3, September, 1995
- [11] KAJARI, M., ČESIĆ, M., Ograničivači uzbude u digitalnoj regulaciji napona sinkronih generatora, Zbornik radova KoREMA 38, 1. svezak, 1993.
- [12] ADIBI, M.M., et al., Optimizing Generator Reactive Power Resources, IEEE Transactions on Power Systems, Vol. 14, No. 1, February, 1999
- [13] ZLATANOVIĆ, D., Solicitare magnetice si termice in dintele frontal statoric turbogeneratoarele de 330 MW, Energetica, Vol.37, No.4-5, 1989 (Rumunjska)
- [14] KHAN, G.K.M., et al., An Integrated Approach for the Calculation of Losses and temperatures in the End-region of Large Turbine Generators, IEEE Transactions on Energy Conversion, Vol. 5, No.1, March, 1990
- [15] SILVA, V.C, et al., A 3D Finite-Element Computation of Eddy Currents and Losses in the Stator End Laminations of Large Synchronous Machines, IEEE Transactions on Magnetics, Vol. 32, No. 3, May, 1996
- [16] ZLATANOVIĆ, D., Cosideratii privind functionarea generatoarelor din SEN in regim subexcitat de durata, Energetica, Vol.34, No.4, 1986 (Rumunjska)
- [17] ZLATANOVIĆ, D., Limitele termice de functionare in regim subexcitat de durata ale turbogeneratoarelor, Energetica, Vol.34, No.2, 1986 (Rumunjska)
- [18] TITOV, V.V., et al., Turbogeneratori - Rascot i konstrukcija, Energija, Lenjingradskoe odelenie, 1967
- [19] ČULIG, Z., et al., Istraživanje elektromagnetskih i toplinskih prilika u sinkronom generatoru u posebnim pogonskim uvjetima, XII Savjetovanje JUKO CIGRÉ, Budva, 1975.
- [20] KURTOVIĆ, M., JAJAC, B., Utjecaj čeonih dijelova na dijagram opterećenja sinkronog stroja, XVII Savjetovanje JUKO CIGRÉ, R.11.21, Budva, 1987.
- [21] LACHS, W.R., SUTANTO, D., A Rotor Heating as an Indicator of System Voltage Instability, IEEE Transactions on Power Systems, Vol. 10, No. 1, Februray, 1995

---

Uredništvo primilo rukopis:  
2007-03-06

Manuscript received on:  
2007-03-06

Prihvaćeno:  
2007-04-02

Accepted on:  
2007-04-02